8-9-2008

A study on biological fuel cells for micro level applications

Duminda Anuradh Gunawardena

A STUDY ON BIOLOGICAL FUEL CELLS FOR MICRO LEVEL APPLICATIONS

By

Duminda Anuradh Gunawardena

A Thesis
Submitted to the Faculty of
Mississippi State University
in Partial Fulfillment of the Requirements
for the Degree of Master of Science
in Biological Engineering
in the Department of Agricultural and Biological Engineering

Mississippi State, Mississippi

August 2008

A STUDY ON BIOLOGICAL FUEL CELLS FOR MICRO LEVEL APPLICATIONS

By

Duminda Anuradh Gunawardena

Approved:

Sandun D. Fernando Assistant Professor of Agricultural & Biological Engineering (Director of Dissertation and Graduate Coordinator)	S. D. Filip To Assistant Professor of Agricultural & Biological Engineering (Committee Member)
Steven H. Elder Assistant Professor of Agricultural & Biological Engineering (Committee Member)	Sarah Rajala Dean of the Bagley College of Engineering

Name: Duminda Anuradh Gunawardena

Date of Degree: August, 2008

Institution: Mississippi State University

Major Field: Biological Engineering

Major Professor: Dr. Sandun D Fernando

Title of Study: A STUDY ON BIOLOGICAL FUEL CELLS FOR MICRO LEVEL APPLICATIONS

Pages in Study: 112

Candidate for Degree of Master of Biological Engineering

Finding new energy sources has been a major quest in the 21st century. The challenge is not simply to find alternatives for traditional energy sources like crude oil and coal to generate power on a large scale but also to produce power to energize micro and nano scale devices. For electricity production in the nano and the micro scale, research has been done on technologies including fuel cells and batteries.

This study is focused on two themes, i.e., the use of a microbial fuel cell and an enzymatic fuel cell for potential bioMEMS/NEMS applications. In the first , a fully functional fuel cell with yeast as the microbe using glucose as the fuel was tested to characterize its performance. In the second phase, a lactate dehydrogenase based enzymatic fuel cell using lactate as the fuel was tested to understand the performance characteristics.

Key words: Biological fuel cell, Microbial fuel cell, Enzymatic fuel cell.

DEDICATION

This thesis is a result of constant guidance, support and love I got from various people through out my life. Its is a great pleasure to dedicate this work to all of them including my dad Kumarajeeva Gunawardena , my mom Maulikantha Gunawardena and my brother Shane Gunawardena, whose support became the impetus behind every single achievement in my life.

ACKNOWLEDGEMENT

I’m sincerely grateful to many who gave me a wonderful support in caring out my experiment . Without their generous support its absolutely difficult for me to think about completing my research successfully. I owe many thanks to my committee. My advisor Dr Sandun Fernando was a mentor to me all through out the years in many respects. His advices not only helped me to stay focused on my objectives but also helped to keep myself in high spirits. Dr. Filip To was a good teacher and also a good friend to me. His support in terms of instrumentation was indeed an asset. Dr Steven Elder guided me for doing literature reviews through his journal review class, which was very beneficial for my thesis work.

I got a wonderful support from many other personals from different departments as well. Dr. David Wipf from the department of chemistry was very supportive to me in terms of electrochemistry related issues I encountered in the experiment. Dr. Dwain Braasch gave me a tremendous help in understanding enzyme chemistries and also was so generous as to let me use his lab for enzyme immobilization procedures.

I should humbly mention the support the department workshop manager, Daniel Chesler gave to me in terms of machining and fabricating my experimental fuel cell. My colleagues in the bio energy research group was always behind me giving a wonderful support from sharing of knowledge to helping with instruments. Among them I would like to give my special thanks to Dr Sushil Adhikari who helped me in various ways.

TABLE OF CONTENTS

LIST OF TABLES

TABLE Page

LIST OF FIGURES

FIGURE Page

CHAPTER I

INTRODUCTION

Abstract

Renewable energy, fuel cells, and nano technology are some key research concepts that evolved during the 21st century. With a lot of emphasis given to protecting the environment and the planet, much of the energy production research has been focused on finding cleaner, environmentally friendly, and renewable energy sources. Hence, bio-based energy sources have gained a significant interest. Biobased energy resources span a wide range including biomass, microorganisms and enzymes. In this continuum, fuel cells, despite being inorganic, have become an attractive power source. Out of numerous fuel cell technologies such as proton exchange fuel cells (PEMFC), solid oxide fuel cells (SOFC), Molten carbonate fuel cells etc, PEMFCs have gained attention, especially for mobile applications since these operate at low temperatures and are fairly versatile. In PEM fuel cells, hydrogen is the fuel and the only byproduct is water. The inorganic catalyst in the anode (compartment) of a PEM fuel cell dissociates hydrogen in order to produce protons and electrons. The electrons are routed via an external circuit to be utilized for useful applications while the protons are transferred to a cathode compartment via a proton conductive membrane where they recombine with electrons transmitted from the external circuit and oxygen to produce water.

Ironically, the inorganic catalysts could be replaced by bio-organic catalysts (called enzymes) or enzyme containing microorganisms which could oxidize a fuel. In biological reactions, generation of protons and electrons are frequent occurrences. For example, microorganisms in their metabolic cycles consume carbohydrates and proceed through a glycolysis reaction for producing energy. This reaction system is comprised of a number of NAD^+/NADH redox cycles where some of the released protons and electrons can be routed through the membrane to the ambient media in an analogous manner to an inorganic PEM fuel cell. Using this concept, a new type of fuel cell known as a "biological fuel cell" was created. The first phase of this study concentrates on using Baker's yeast (Saccharomyces cerevisiae) as a living biocatalyst in a microbial fuel cell. Further studies on the metabolisms in the microorganisms indicated that instead of microorganisms, enzymes that are involved in the process alone can do the fuel oxidation much better. As the enzymes are substrate specific these are an excellent choice for a fuel cell that runs on a specific fuel substrate. (As a result a new branch of biological fuel cells was originated as enzymatic fuel cells.) The second phase of this study deals with looking at the possibility of developing a fuel cell for in-vivo applications using lactate, a substrate found in human blood using lactate dehydrogenase as the enzyme.

In this study performance characteristics of a biological fuel cell and an enzymatic fuel cell were compared in order to understand the dynamic behavior of these distinct fuel cell systems. Yeast was selected as the microorganism in the microbial fuel cell and glucose was selected as the fuel. The electron transfer from the species to the electrode was promoted by using a mediator. Therefore it was hypothesized that when methylene blue is used as the anode mediator in the anode compartment where the microorganism is

kept and potassium ferricyanide is used in the cathode as the cathode mediator, a superior fuel cell could be developed in comparison to a control where no mediators were used. Armed with the knowledge obtained while developing the yeast based fuel cell, a second study was performed on a miniaturized version of a fuel cell targeted for implantable applications. The ability to generate power from within the body to energize implantable devices, such as cardiac pacemakers or micro drug delivery devices, would be unprecedented and highly desirable for the development of future biomedical industry.

In the second experiment the enzymatic fuel cell was designed for targeting the lactate present in blood. Lactate dehydrogenase (LDH), an oxidoreductase enzyme, oxidizes lactate to pyruvate. It was hypothesized that a fully functional enzymatic fuel cell could be developed by immobilizing LDH on a gold anode and a platinum cathode.

History of Bio Fuel cells

In 1963, W. Mitchell wrote, "Perhaps the most refined fuel cell system today is the human body, a mechanism that catalytically burns food in an electrolyte to produce energy some of which is electrical"[1, 2]. Also, the experiment conducted by the biologist (Lugi) Galvani in the 1780s using a frog leg, established a connection between electrical energy and biology [3]. The first indication that organisms can generate voltage and deliver a current was inspired by Michael Cresse Potter, a botanist [4]. In the early part of the 19th century different organisms like bacteria, algae, and yeast had been used in this type of research. With the advent of space exploration, a considerable amount of attention has been given to developing concepts on utilization of waste water to harness electricity. In light of this, microbial fuel cells based research received renewed attention during the

sixties and the early seventies. Coupled with ever increasing crude oil prices, all areas of alternative energy have gained momentum including the area of biological fuel cells [5, 6].

Bio-fuel cell defined.

A fuel cell is a device which converts the chemical energy present in a fuel to electrical energy. Biofuel cells possess several key attributes: the catalysts as well as the fuel/s used are renewable. Major advantages of biological fuel cells are their fuel flexibility and the ability to perform at low temperatures. Inefficiencies associated with the oxidation reaction of fuels and mass/charge transfer limitations are major challenges that need to be overcome before commercial use of biofuel cells becomes feasible. Recent research on biofuel cell technology is mainly targeted towards overcoming these technological challenges. In a classical process of power generation, four main processes can be identified:

(a) Combustion of the fuel which converts the chemical energy into heat.

(b) The heat generated is used for steam generation.

(c) The steam generated is fed into a turbine.

(d) Mechanical energy is converted to electricity.

However, a fuel cell, as a single entity, bypasses all of the above four steps and produces electricity as long as a continuous supply of fuel is present. The time lines of fuel cell development is shown in the Figure 1.1. Despite some uncertainty, Sir William Grove (1839) and the Swiss scientist Christian F. Shoenbein are regarded as the first to develop a fuel cell. The oxidation in a fuel cell occurs at the anode releasing electrons to the electrode and the reduction takes place at the cathode where the electrons that

traveled through an external circuit are collected and combined with the terminal electron acceptor - which is in most cases is oxygen to produce H_2O. There are different types of inorganic fuel cells in use and can be grouped according to the electrolyte used as shown in Table 1.1.

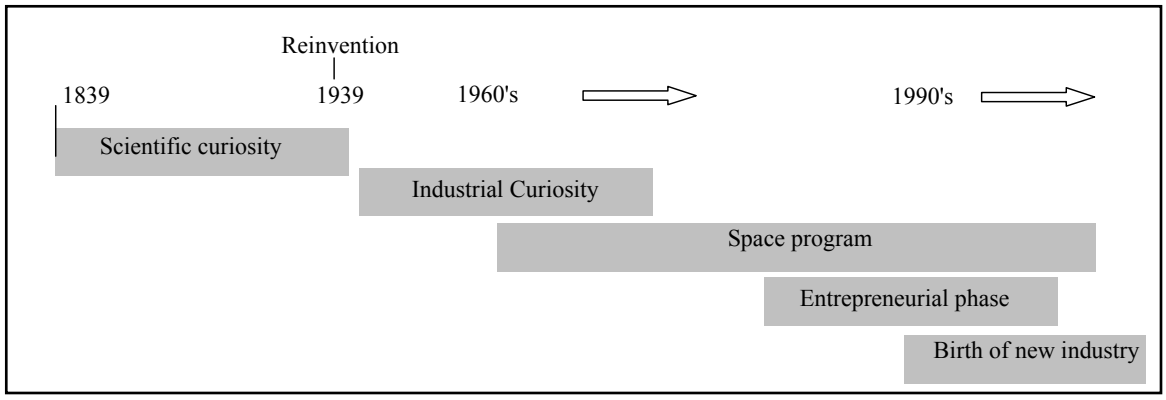

Figure 1.1. The time line of the fuel cell development[7].

Table 1.1. Different types of fuel cells that has been tested.[7]

Alkaline fuel cell (AFC)	KOH as the electrolyte and electro catalysts such as Ni, Ag, Metal Oxides
Polymer electrolyte membrane fuel cell (PEMFC)	Proton conductive polymer membrane as the electrolyte and Pt as the catalyst
Phosphoric acid fuel cells (PAFC)	Concentrated phosphoric acid as the electrolyte and Pt as the catalyst
Molten carbonate fuel cell (MCFC)	Has a combination of alkali metals (Li, K, Na)
Solid oxide fuel cells (SOFC)	Non porous metal oxide (YSZ) as the electrolyte

The biological fuel cells (BFC) use enzymes or micro organisms as catalysts for the oxidative reactions that takes place at the anode. Substrates for biological fuel cells

vary according to the microbe or enzyme used. For example, glucose is a common fuel that is tested as a substrate in low temperature fuel cells. Other renewable fuels include alcohols, acids, waste water and biomass.

Fuel cell performance measurements.

Performance parameters are very important in comparing effectiveness of various fuel cell designs. The typical performance parameters monitored in fuel cell studies are given in the Table 1.2.

Table 1.2. List of parameters for fuel cells.

Equation	Parameter
E_{oc}	Open Circuit Voltage (The terminal potential when there is no current through the cell)
E_{cc}	Closed Circuit Voltage
I_l	Load Current
R_i	Internal Resistance
$E_{oc} = E_C - E_A$	The open circuit voltage {The voltage difference of the individual potentials of anode (E_A) and cathode (E_C)}
$Ecc = Eoc - I_l R_i$	The closed circuit voltage
$P = E_{cc} I_l$	The power of the cell
$\eta = \frac{RT}{zF} Ln \frac{[OX]}{[RE]}$	Electrode over potential { Gas constant (R), Temperature (T), Faraday constant (F), No. of electrons (z), Concentration of oxidized and reduced species [OX], [RE].}

Classifications of Biological fuel cells

The biological fuel cells (BFC) can be categorized into two main types (i) Microbial fuel cells and (ii) Enzymatic fuel cells. The fuel cell reactions that are catalyzed by microbes are referred to as microbial fuel cells. On the other hand, if the catalyst is an enzyme, such fuel cells are referred to as enzymatic fuel cells. The main function of the biocatalyst in the fuel cell is to catalyze the oxidation of the organic substrate which is typically glucose or sugar. The catalyst used in a bio-fuel cell could be simply an organism like Bakers yeast or some improved microbial species like *R. ferrireducens*.[8-10].

Biological fuel cells involving microorganisms

In microbial catabolism, under anaerobic conditions, carbohydrates are oxidized without the presence of the oxygen. This oxidation reaction gets partially completed inside the microbial cellular structure and with the help of co-enzymes, the electrons and the protons are transferred outside the cellular membrane. The overall reaction can be simplified as given in Equation 1.1.

$$C_6H_{12}O_6 + 6O_2 \longrightarrow 6CO_2 + 6H_2O \quad (1.1)$$

$$C_6H_{12}O_6 + H_2O \longrightarrow 6CO_2 + 24H^+ + 24e^- \quad E^{\Theta} = 0.014V \quad (1.2)$$

$$O_2 + 24H^+ + 24e^- \longrightarrow 12H_2O \quad E^{\Theta} = 1.23V \quad (1.3)$$

$$C_6H_{12}O_6 + 2NAD^+ + 2ADP + 2PO_4^{-3} \longrightarrow 2NADH + 2ATP + 2\,pyruvate \quad (1.4)$$

In the absence of oxygen glucose is converted to CO_2 using the reaction given in Equation 1.2. These electrons will be transferred to the anode through an external circuit and the H^+ will travel to the cathode compartment through the proton exchange membrane. The electrons that came through the external circuit as shown in Figure 1.2, will combine with the O_2 and H^+ to form water according to the Equation 1.3.

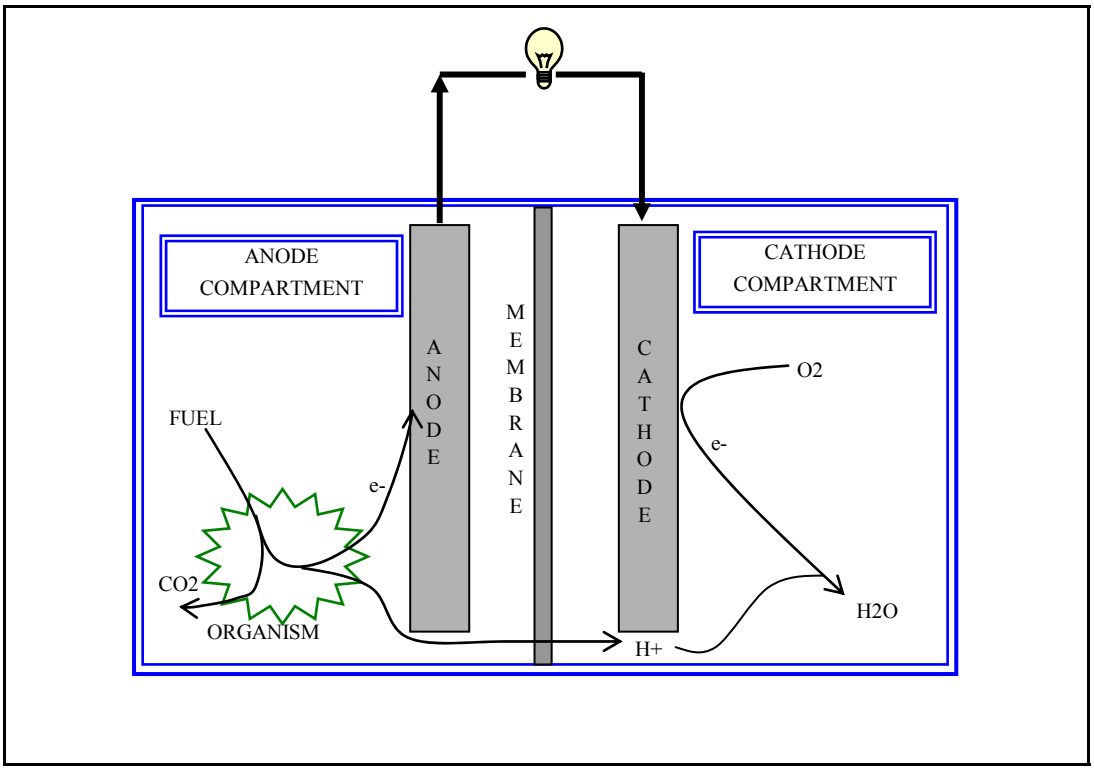

Figure 1.2. Schematic diagram of a Biological fuel cell and its functions.

In a microbial fuel cell, the electron and the proton generation takes place inside the cell membrane where a number of enzyme reactions are ongoing. The microbes consume glucose to generate energy to sustain their life. This energy is generated by the oxidation of glucose. The glucose oxidation can take place under two conditions: with

oxygen (respiration) or without oxygen (fermentation). The glucose under aerobic oxidation follows four distinctive steps as given below [11].

1. Glycolysis
2. Krebs cycle
3. Electron transport chain
4. Oxidative phosphorylation

In glycolysis, which is also known as Embden Mayarhoff pathway, the six-carbon glucose atom is broken down into two molecules of pyruvate as given in Equation 1.4. This takes place in 10 steps and each of which is catalyzed by a specific enzyme. The pyruvate formed in the glycolysis would go further through a three stage process where it would finally end up as CO_2 and energy in the form of ATP. The total ATP production from glucose in respiration is given in the Table 1.3.

Table 1.3. The ATP yield for corresponding reaction.

Reaction Sequence	ATP Yield
Glucose $\longrightarrow$ Fructose 1,6-diphosphate	-2
2 Trios phosphate $\longrightarrow$ 2,3-phophoglyceric acid	2
$2NAD^+ \longrightarrow 2NADH \longrightarrow 2NAD^+$	6
2Phosphoenolpyruvic acid $\longrightarrow$ 2 pyruvic acid	2
2 pyruvic acid $\longrightarrow$ 2 acetyl CoA + $2CO_2$	
$2NAD^+ \longrightarrow 2NADH \longrightarrow 2NAD^+$	6
2Acetyl CoA $\longrightarrow$ $4CO_2$	24
Net : $C_6H_{12}O_6 + 6O_2 \longrightarrow 6CO_2 + 6H_2O$	38

Even though respiration is the main form of energy generation technique in organisms, some can generate energy under anaerobic conditions as well. Under anaerobic conditions, glucose will be converted to pyruvate similar to aerobic pathway, but, in the next stage, the Krebs cycle will not follow. Depending on the organism – prokaryote / eukaryote - a specific pathway will follow .Yeast for instance will make alcohol fermentation and some organisms follow the lactic acid fermentation instead. Since the ATP production is very less under anaerobic conditions - which is almost two molecules per one pyruvate molecule, the organism needs rapid processing of NAD^+ and NADH to generate adequate energy.

For the purpose of harvesting H^+, what matters for a Bio Fuel cell is the amount of coenzyme (NAD) that gets involved in the reaction. In that perspective, the anaerobic reaction is much favorable for proton harvesting compared to aerobic conditions as under anaerobic conditions NAD+ / NADH production takes place at a significant speed where as oxygen would not combine with H^+ generated from NADH oxidation short circuiting the fuel cell cathode half reaction.

Different categories of Microbial Fuel Cells

Out of various types of Biological Fuel Cells designs that have already been tested, four main categories could be identified.

- The uncoupled bioreactor MFCs : A separate compartment where organisms produces the hydrogen and the hydrogen is fed into a hydrogen fuel cell
- Integrated bioreactor MFCs: The hydrogen production and the electricity generation both take place in the same chamber

- The MFCs with mediated electron transfer: where intermediate molecules are shuttling electrons from the organism's body to the electrode
- The MFCs with direct electron transfer: special types of modified species where electron transfer to the electrons take place without the presence of any mediator molecules..

The first two are quite similar in design and possess the same limitations that a chemical fuel cell has. The bioreactors that convert oxygenates like glucose directly into hydrogen is not very efficient due to fast inhibition of enzymes by evolving Oxygen. Theoretical output has been limited 10%. Another shortcoming of the system is that the H_2 produced is not pure and it could contain traces of CO and H_2S. There are different types of bacteria and algae that generates hydrogen under anaerobic conditions, e.g. *Escherichia Coli, Enterobactor ,C. Butyricum.*

The second fuel cell type - Integrated Bioreactor MFC is similar to the one described above apart from the position of the reactor [12, 13]. These fuel cells typically use Pt as the anode catalyst. The third type uses intermediate molecules known as mediators to facilitate electron transfer [14]. The mediators shuttle electrons between the electrode and the redox enzyme in the microorganism [15].

$$C_6H_{12}O_6 + \text{Mediator}_{(O)} \longrightarrow \text{Product} + \text{Mediator}_{(R)} \quad (1.5)$$

$$\text{Mediator}_{(R)} \longrightarrow \text{Mediator}_{(O)} + \text{Electrons} \quad (1.6)$$

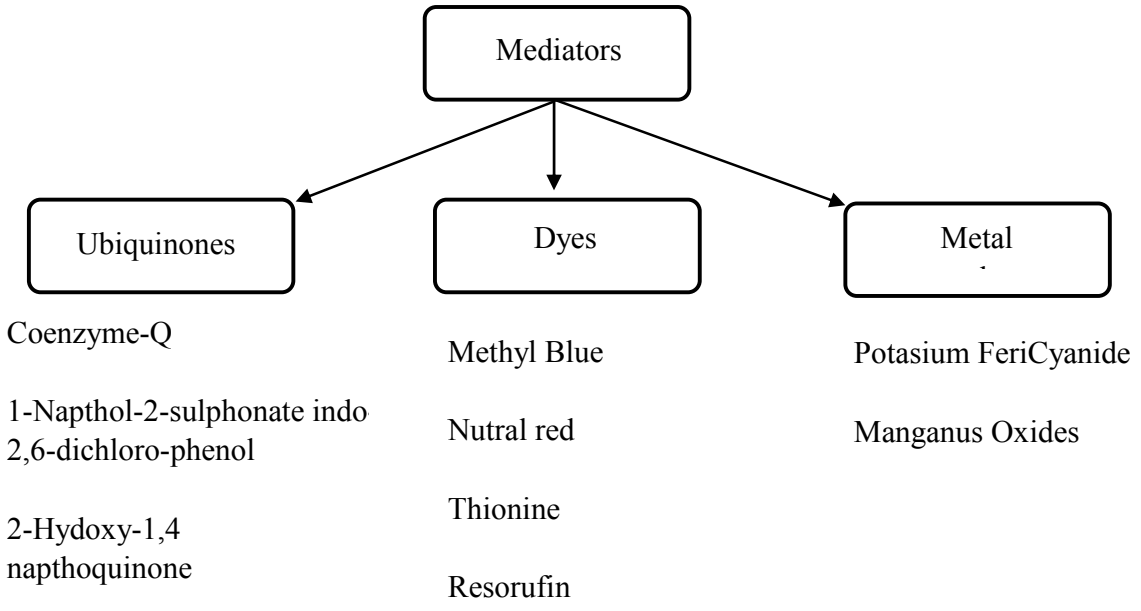

Figure 1.3. Different types of mediators used in fuel cells.

There are a vast number of mediators tested in microbial fuel cells and many of which are dyes. The dyes have the potential to stain the cell membrane and thus they extract the electrons from the NAD^+ / NADH redox cycle. The Figure 1.3 shows some of the mediators that has been used in the MFC's so far. The mediator at the microorganism will get reduced as shown in the Equation 1.5 . This reduced mediator finally will reach the anode where it will undergo oxidation , resulting in a reaction given in Equation 1.6. The characteristics a mediator should possess has been well documented and are as follows [16, 17]:

- Mediators are redox molecules which can form redox couples.
- The mediator molecules should be stable in both redox and the oxidized form
- It should not be biologically degradable

- It should not be toxic to the biological species.

However, practically, many of the mediators are prone to biodegradation and in many cases are toxic to living organisms at high concentrations [18, 19].In the mediatorless fuel cells, the bacteria would interact with the electrode directly with self-made mediators. Experiments have been conducted on bacteria that reduces Fe(III), such as *Shewanella Putrefaciens* , *Geobactor Sulferreducens* , *Rhodeferax ferrireducens* [20] which are examples for mediator producing microorganisms.

Characteristics of different Organisms

Some of the microorganisms together with their reported open circuit voltage (OCV) is shown in Table 1.4. Different bacteria cultures have been reported to have experimented and they can be categorized into two forms as axenic, which is a pure bacteria culture and the mixed culture which doesn't consists of a pure micro organism as shown in Figure 1.4.

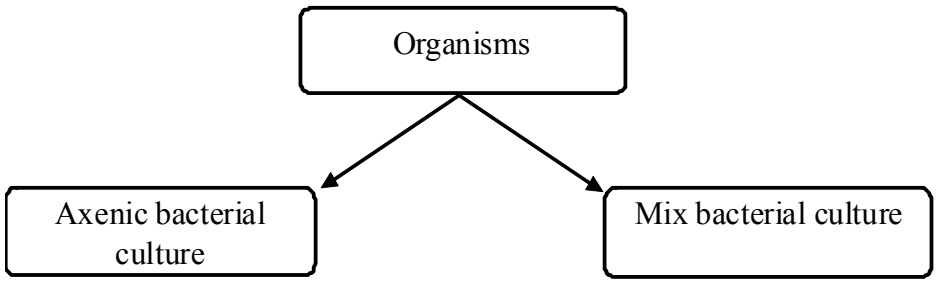

Figure 1.4. Differentiation of organism with respect to their purity.

Table 1.4. Different Organisms and some results

Microorganism	Substrate	Electrode	Mediator	OCV (V)
Proteus vulgaris	Glucose	graphite felt	Thionine	0.7
E. Coli	Glucose	graphite felt	Neutral Red	0.85
A. succinogenes	Glucose	graphite felt	Thionine	0.85
Rhodeferax ferrireducence	Glucose	graphite rod	N/A	
Clostridium butyricum	Starch / Glucose	graphite felt		0.759
Desulphovibrio desulphuricans	Lactate and pyruvate	activated carbon	Sulphate	N/A
Shewanella putrefaciens	Lactate	carbon felt	Mn+4	0.5

Microbes are the power generators of a fuel cell and the selection of the microorganism should be done according to the following criteria:

- Significant growth rate
- High substrate specificity
- High energy transfer efficiency

In practice, it is very difficult to maintain axenic conditions as the purity of the culture become compromised by contamination with undesired bacteria. The mixed cultures have shown improved performances with this regard [21].

The internal resistance of a Fuel Cell

The internal resistance of a fuel cell plays an important role in determining the practicality of a fuel cell. When the internal resistance is high, the power loss inside the

cell is significant and thus reduces the output voltage available at the end terminal [7, 22]. Some factors that affect the fuel cell voltage loss are as follows:

- Kinetics of the electrochemical reaction
- Internal electrical and the ionic resistance
- Difficulties in getting the reactant to the reaction site.
- Internal current
- Crossover of reactants.

The polarization curve of a typical fuel cell is given in Figure 1.5. The section 'A' of the Figure 1.5 depicts the activation loss.

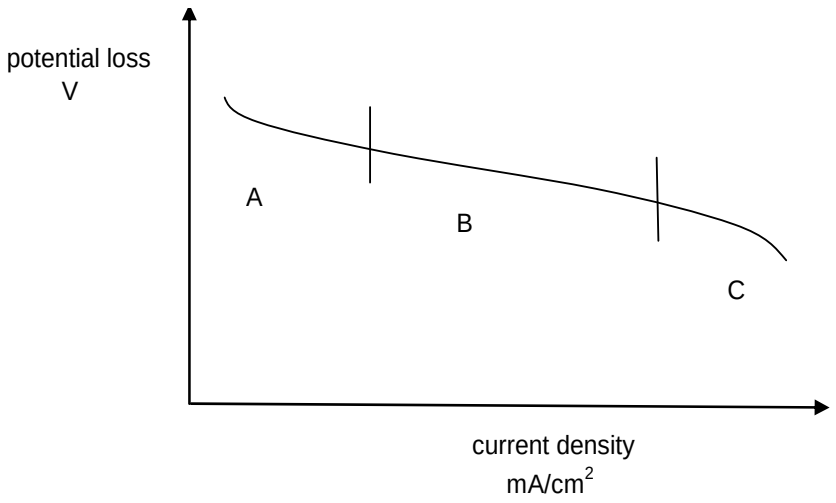

Figure 1.5. The polarization curve for a typical fuel cell.

A voltage difference from the equilibrium is needed to carry the reaction forward and is termed as activation over potential. The reason for the over potential is because the oxidizing or the reducing reactions of the cell needs some energy to activate the reaction.

$$\Delta V_{act} = a + b \,.\, \times Log(i) \qquad (1.7)$$

This loss is present at both the anode and the cathode and typically, the cathode over potential is much larger than the anode and with the increased exchange current density this over potential can be reduced [7, 22]. This loss can be explained from the Tafel equation as given below in Equation 1.7. Where ΔV_{act} = overpotential, i = current density, $a = -2.3\frac{RT}{\alpha F}\log(i_o)$, $b = 2.3\frac{RT}{\alpha F}$, R = gas constant, i_o= exchange current density, T = temperature, F = Faraday constant and α = transfer coefficient.Some measures that can be taken to minimize the activation over potential loss would be as follows.

- Increasing the operation temperature.

In an inorganic fuel cell, raising the temperature would reduce the activation over potential but in a microbial fuel cell or an enzymatic fuel cell, it's not possible to increase the temperature unless the bio-reaction part is separate from the anode chamber.

- Decreasing the activation loss at the electrode surface.

The activation potential can be decreased by adding a catalyst to the electrode. The catalysts that have been tested (for example Pt) was reported to be get polluted by bacterial suspensions. However, covering the electrode with a conductive layer has proven to be successful [23]. In addition to Pt, manganese oxide has also been attempted for this purpose [16, 24]. Increasing the surface area is another way to decrease the activation potential therefore when the surface area is increased, the current density gets reduced.

- Decreasing the activation losses at the bacteria

Using the correct mediator would eliminate this problem. Mediators would travel through the cell membrane reducing the activation losses inside the cellular structure.

The loss of potential due to internal current and cross over of reacting gasses through the membrane would also be significant if the fuel cell is operating at low current densities. The membrane is not impermeable to the oxygen molecule as certain percentage can be diffused into the anode resulting in lowering the current in the circuit. Some electrons with the help of an electron shuttle will find its way to the cathode creating a loss in the circuit current.

The effective current through the external circuit (I_{ext}) can be related to the current generated (I) and to the internal current loss in the cell (I_{loss}) as given in the Equation 1.8. The portion of the graph in the Figure 1.5 marked as "B" represents the ohmic loss of the fuel cell. This is due to the resistance that ions face in the electrolyte. In this region of the graph the potential drop (ΔV) is related to the circuit current (I) and the internal resistance (R) as shown in Equation 1.9. The internal resistance (R) contains three types of resistances namely ironic, electronic, and contact resistance. Both the electronic resistance and contact resistance would be negligible compared to ionic resistance if the graphite electrodes were used [7].

$$I_{ext} = I + I_{loss} \qquad (1.8)$$

$$\Delta V = I \times R \qquad (1.9)$$

The 'C' section of the graph represents the concentration polarization losses of the fuel cell. This takes place due to depletion of the reactants at the anode faster than they

can be transported to the electrode. This happens when larger currents drawn. Usually in Biological fuel cells the currents drawn would not be of higher values and this is not a significant problem anticipated.

There is very little work done on internal resistance of biological fuel cells. However, data on power, current, and voltage values for different loading conditions are abundant. In many instances, at high loads it can be inferred that the internal resistance of the cell should also be significantly high.[25-27]. One main thrust of our study was understanding the behavior of internal resistance values in biological fuel cells which is an existing knowledge gap.

Enzymatic fuel cells

The use of microorganisms to catalyze the oxidation of a substrate dictates strict ambient conditions even though it triggers numerous physiological processes with lessened specificity [28]. Having specificity is an attractive property that the enzymes posses in catalyzing oxidative or reductive reactions. For electrochemical fuel cell reactions, having specificity is a fundamental requirement. Therefore, the use of enzymes in such applications can be seen quite advantageous [29-32]. Enzymatic fuel cells research has branched out from extensively researched bio-sensor studies where the substrate specificity of the redox enzymes are exploited to produce electricity [6, 33, 34]. However, the use of enzymes for fuel cell applications posses a number of difficulties.

Especially because enzymes are very sensitive for the physiological conditions and they are fairly expensive compared to the microorganisms due to laborious extractive processes. In addition, the enzyme structure can make electron communication fairly

difficult with the electrode [35, 36]. Usually enzymes contain a hydrophilic protein surface covering a hydrophobic active center where the catalysis takes place. While some enzymes having easily accessible active centers and diffusive co-factors, some have tightly bound co-factors hidden deep inside their protein structure.

Depending on its makeup, the electrical communication with the electrode can vary significantly among different enzymes [37, 38]. Different classes have emerged within fuel cell research based on the structural properties of the enzymes used. The enzymes that can be used in a fuel cell falls under the oxidoreductases where the dehygonases and the oxidases are the most used categories. About a large percentage of oxidoreductases have NADH as the co-factor (eg. lactate dehydrogenase). The NADH has a great degree of mobility whereas some other enzymes like glucose oxidase (GOX) has a tightly bound FAD cofactor shown in Figure 1.6.

Glucose oxidase is an enzyme where its active center is hidden deep inside the protein structure where the electrical communication with an electrode is impossible unless it is properly wired or attached to the electrode [35, 36, 39]. This opens up two classes of enzymes for the fuel cell applications , (i) the direct electron transfer (ii) the mediated electron transfer.

Direct electron transfer

When the enzyme catalyses the redox reaction of the substrate near the electrode the electrons will be exchanged directly between the electrode and the enzyme active center. Studies have indicated that there are a number of enzymes that posses the property of direct electron transfer with the electrode[40].

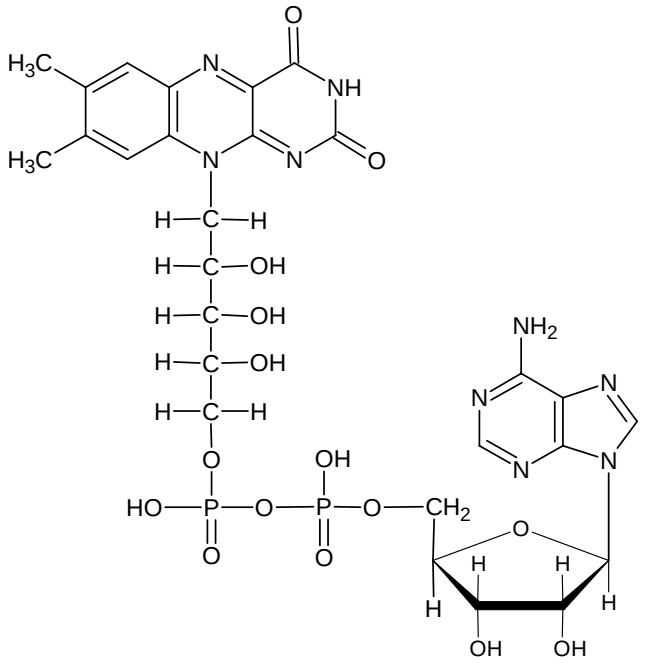

Figure 1.6. The molecular structure of FAD.

The steps involving the electron transfer to the enzymatic electrode has been identified as follows [41]:

a) Diffusion of reactant protein to the electrode surface.

b) Association of protein with the electrode surface in an orientation suitable for electron transfer.

c) Electron transfer.

d) Dissociation of protein from the electrode surface.

e) Diffusion of product protein away from the electrode surface.

Some of the oxidoreductases as it has been reported having this property are: laccase, lactate dehydrogenase, hydrogenase, methylamine dehydrogenase, lactate dehydrogenase, succinate dehygrogenase, fumarate reductase, D-fructose dehydrogenase,

alcohol dehydrogenase, and D-gluconate dehydrogenase [42, 43]. Laccase among peroxidases has attracted much attention since the active center which contains a Cu cluster catalyzes reduction of oxygen to H_2O. Since the active center is located at the periphery of the protein structure it can readily accept the electrons upon contact with an electrode [44]. The challenge posed by this type of electron transfer is to have the right orientation of the enzyme for the electron transfer to occur at the electrode. Further, it has been reported that the laccase has been tested for direct electron transfer with an electrode modified with 4-aminothiophenol. This modification has proven to be effective as compared to various other types of monolayers that were tested on the electrode [45].

Mediated electron transfer

Even though direct electron transfer looks simple, complexities exists when getting the enzyme into right orientation to facilitate electro transfer between the substrate and the electrode. To circumvent these difficulties, enzymes that have diffusible cofactors present in its protein matrix (like NAD^+ which is shown in Figure 1.7) or artificially introduced molecules like bensile viologen has been reported to be successful[46, 47]. Mediated electron transfer can be further categorized into following: (i) Electron transfer with mobile mediator/s (ii) Electron transfer with immobilized mediator/s.

Electron transfer with mobile mediators

A large number of oxidoreductases have NADH as the co-factor and they are fairly loosely bound and has the flexibility to diffuse away from the enzyme[48]. Therefore, the NADH can act like a natural mediator for the electron transfer in a fuel

cell. However, having NADH as the electron transfer molecule at the electrode poses some serious issues.

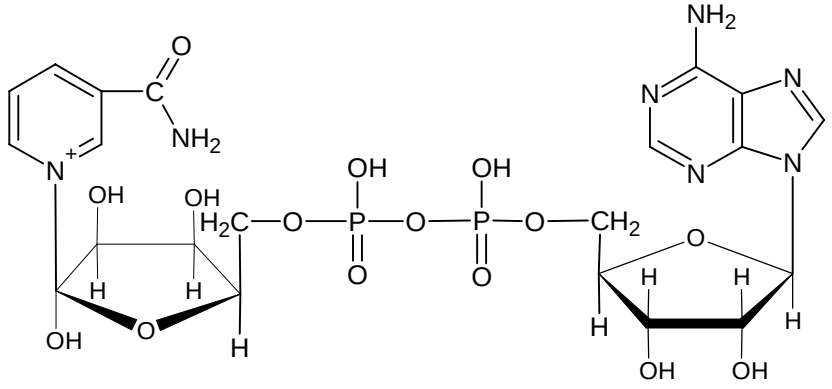

Figure 1.7. The molecular structure of NAD^+.

As this reaction involves two steps in the process of electron transfers, any intermediate molecule produced should remain stable until it complete the reaction by transferring the second electron[35]. NADH should not diffuse away from the enzyme and the electrode or in other words it should stay intact between the electrode and the enzyme and also, $NADH/NAD^+$ should not hydrolyze rapidly [49]. The over potential of the oxidation of the NADH also play a critical role. It should not be very high to initiate side reactions. Studies have indicated that the thermodynamic redox potential ($E^{\circ'}$) of $NADH/NAD^+$ is around -0.56V vs. saturated calomel electrode (SCE) at pH 7.0. And also the electrochemical studies have further been able to reveal that the oxidation of this co-factor at the surface of the electrode is highly irreversible and has large overpotentials such as 0.4V , 0.7V , and 1V vs. SCE at carbon , Pt and Au electrodes respectively [35, 50]. Consequently, adsorption of NADH / NAD^+ on to the electrodes such as Au , Pt or carbon can inhibit the oxidation process or poison the electrode surface. Some times the

adsorbed NADH can be oxidized to undesirable products which can lead to the degradation of the functionality of the co-enzyme. For these reasons it is not reasonable to depend on natural mediators for the electron transfer between the electrode and the enzyme. An intermediate molecule has to be found which can re-oxidize the NADH back to NAD^+ [51]. Different artificial mediators have been successfully attempted in the enzymatic fuel cells (eg. Benzyl viologen (BV), 2,2-azinobis(3-ethylbenzothiazoline-6-sulfonate) known as ABTS, ferrocene monocarboxylic acid (FMCA), N,N,N,N –tetra-p-phenylenediamine (TMPD), syringal diazine, and $K_3Fe(CN)_6$ / $K_4Fe(CN)_6$, I_2 /I_3^-).

It has been reported in the literature that the use of enzyme diaphorase to catalyze the re-oxidation of NADH in the presence of benzyl viologen has been successful. In this case, benzyl viologen acts as the mediator that transfers electrons to the electrode. In this particular experiment conducted by Palmore methanol was oxidized to carbon dioxide producing NADH in a series of steps using three enzymes alcohol dehydrogenase, aldehyde dehydrogenase, and formate dehydrogenase. A Pt cathode has been used to reduce oxygen to water in the fuel cell. At ambient conditions of pH 7.5, the fuel cell has generated a power density of 0.67mW/cm^2 at 0.49V [47]. Further on alcohol fuel cells, the electrode has been modified with different polymers in order to facilitate the electron transfer. In alcohol fuel cells, specific dehydrogenases have been used at the anodes to oxidize alcohols such as methanol, ethanol, propanol, and butanol [52, 53].

A direct methanol fuel cell where methanol dehydrogenase from the species *Mehtylobacterium extorquens* has been used where they have been able to generate an open circuit voltage of 1.4V, a current density of 0.38mA/cm^2 and a power density of

0.25mW/cm^2 with the aid of TMPD as the anode mediator. The anode mediator which was mobilized in the anode is reported to have a half life of 5 days [54].

An oxygen glucose bio fuel cell has similarly been tested with FMCA in the anode compartment and ABTS on the cathode side. In this fuel cell, glucose oxidase has been used as the enzyme to catalyze glucose in which the co-factor FAD is tightly bound to the protein structure making it necessary to have a mediator in order to transfer electrons to the electrode. On the cathode, the enzyme laccase has been used to catalyze the reduction of oxygen to water. ABTS has been used as the diffusional mediator and it has generated an open circuit voltage of 410mV and a short circuit current of 1μA. ABTS can also be used as a substrate for the enzyme bilirubin oxidase where these enzymes oxidize the $ABTS^{-2}$ to a $ABTS^{-1}$ at a redox potential of 0.62V vs. standard hydrogen electrode (SHE). ABTS has further been used by many other researchers in similar applications [55].

Laccase from *Pyricularia oryzae* has been used in another experiment for reduction of oxygen where ABTS was used as the mediator [47]. In this experiment, they have been able to obtain an open circuit potential of 530mV vs SCE and 100μA/cm^2 was drawn at 400mV vs. SCE. The behavior of ABTS with other oxygen reducing enzymes like bilirubin oxidase (BOD) has also been documented [56, 57]. Laccase and BOD both have Cu cluster in its active center. When ABTS participates as the mediator, its redox potential appears to be below the redox potential of the Cu cluster of laccase. But it matches well with BOD. BOD from *M. verrucaria* has been reported in literature to have been used to catalyze the reduction of O_2 with ABTS as the cathode mediator. According to this study current density of 40μA/cm^2 was observed for an ABTS

concentration of 0.25mM. It has been revealed that the current density is positively correlated with ABTS concentration. At 1.5mM concentration, the fuel cell produced a current density exceeding 100μA/cm^2. The Mechaelis Menton parameters for the system as they have reported were k_{cat} = 820/s and K_{ABTS} = 11μM [57]. However, serious draw backs of ABTS has been reported. One such is said to be the oxidative degradation it suffers for potentials larger than 0.98V vs SHE. Despite all these ABTS is still attractive due to its high diffusion coefficient (D_{ABTS} = 3.2 x 10^{-6} cm^2/s) compared to some other redox polymers[57].

Electron transfer with immobilized mediator

Many enzymes lack the ability to make direct electrical contacts between the redox center and electrodes due to the insulative nature of the protein matrix. Glucose oxidase is a good example of an enzyme which has its redox center trapped deep inside the protein structure.

Therefore, special techniques have to be employed to make electrical contact between the enzyme and the electrode [58]. In addition, having diffusional mediators in a fuel cell would require membranes separating the anode and the cathode compartments [39, 59, 60]. Membranes separating the compartments significantly reduce the diffusional flux of reactants on the electrodes. In a biofuel cell such limitations of diffusion is detrimental to the performance as membranes would increase losses within the fuel cell [17, 60]. Immobilization of the mediator on to the electrode can eliminate these issues significantly. Different immobilizing methods have been developed either based on physical or chemical methods. Most of the work on fuel cells found in the literature is on

physical immobilization techniques such as adsorbing the enzymes on to conductive support such as carbon or graphite [27, 61]. Immobilization of mediators onto a surface can improve the conductivity of electrons with the electrode surface as mediators or the enzymes will stay at close proximity from the electrode.

Immobilization is helpful to extend the longevity of the enzymes. A biofuel cell with GOX and BOD immobilized in a redox polymer matrix is reported to have survived as long as 20 days. Even more interesting life spans have been reported when Nafion membrane modified with tetrabutylammonium bromide is used to immobilize dehydrogenases. Generally, the half life of the dehydrogenase is only 7~8hrs. in a solution while lifetime in immobilized enzyme assemblies were reported to be more than 45 days [56, 62]. Immobilization methods of the electro active species can be categorized as follows: (i) Surface immobilization of electro active species (ii) Entrapment of electro active species in to a polymer network.

Surface immobilization of electro active species

The attachment of redox mediators to self assembled mono layers on electrode surfaces has an important advantage. They are highly important for the preparation of multi-component organized systems such as sensors[58, 63, 64].The covalent attachment of enzymes on to an electrode involves mainly three steps. First step is the surface functionalization of the electrode. In this step a hydroxyl groups will be formed on the surface. The noble metal like Au and Pt do not have hydroxyl groups and they have to be prepared by a chemical or electrochemical method [65-70]. A carbon surface with chemical pretreatment can be functionalized with groups like carboxylic, carbonil,

hydroxyl etc. A surface treatment is an important step in the surface immobilization of proteins such as enzymes. The density of the functional groups like hydroxyl groups on the electrode surface determine density of the subsequent layers[71-73]. Extensive research work can be found on self assembly of thiols, disulfide, and sulfides monolayers on metal electrode surfaces like Au, Pt , Ag [74-78]. The covalent attachement of enzymes on to an electrode involves mainly three steps as shown in Figure 1.8. First step in it is the surface functionalization of the electrode where a hydroxyl groups will be formed on the surface.The second step in electrode modification is to attach the mediator molecule. In this, pyrroloquinoline quinone (PQQ), can be covalently attached to the amino group of a cystamine mono layer assembled on a gold surface. This type of an electrode has demonstrated good electro catalytic activity for NADH oxidation, particularly in the presence of calcium ions [79]. The electrochemical studies of PQQ has been well documented. For example, in one study, PQQ has been studied in immobilized states on an Au electrode which was functionalized with a self assembled mono layer. When the mediator PQQ is in diffusional nature it has been reported that, there exists an electrochemically reversible reaction on a cystamine modified electrode.

The electrochemical reduction of PQQ is completely irreversible on a pure Au electrode. Even with the electrodes with negatively charged groups PQQ has demonstrated a highly irreversible characteristics. Also, the amine group of cystamine monolayer on a Au electrode surface has been used as a basis for the covalent immobilization of PQQ with the help of zero length carbodiimide molecule coupling the carboxylic groups of PQQ with the surface amino groups. The electrochemical reaction of the immobilized PQQ is reported to be reversible over a wide pH range. The surface

concentration of the monolayer prepared on the Au electrode in the above way is said to be around $1.0x10^{-10}$mol cm^{-2} and an electron transfer rate constant k_s is around 3.3 s^{-1} (pH 7.0) and the redox potential E^0 for the mobilized PQQ is -0.125±0.003 V vs SCE [80]. Once the mediator part is assembled, the subsequent molecules such as NADH or $FADH_2$ can be assembled. This method can be found in various work presented so far[58, 81-83]. For example, for the enzymes in the dehydrogenase family this method can be very well adopted for immobilization .

There has been a study based on NAD^+dependent lactate dehydrogenase (LDH) which has been assembled onto a monolayer of PQQ-NAD^+. This redox active monolayer has been assembled by covalent attachment of PQQ to a cystamine which was preassembled on to the Au electrode. Then the covalent linkage of *N*6-(2-aminoethyl)-NAD^+ to the PQQ monolayer was followed. The surface coverage of PQQ - NAD^+ layers is said to be around 1.2 $x10^{-10}$ mol cm^{-2} whereas the surface coverage of LDH bound to the redox active monolayer was around 3.5 $x10^{-12}$ mol cm^{-2}. The assembled LDH monolayer was active in the bio-electro catalytic oxidation of lactate. But there is no report of the turn over rate regarding the composite enzyme assembly in this work. The bio-electro catalyzed process involves the PQQ-mediated oxidation of the immobilized NADH in the presence of Ca^{2+} ions [84]. The LDH linked to the PQQ-NAD^+ monolayer assembled on the electrode surface showed moderate stability. It has been detected that the biocatalyst has dissociated to the solution. This is a critical issue and usually avoided by cross linking the enzymes with glutaric dialdehyde. There has been a similar work done with malate dehydrogenase and glucose oxidase.

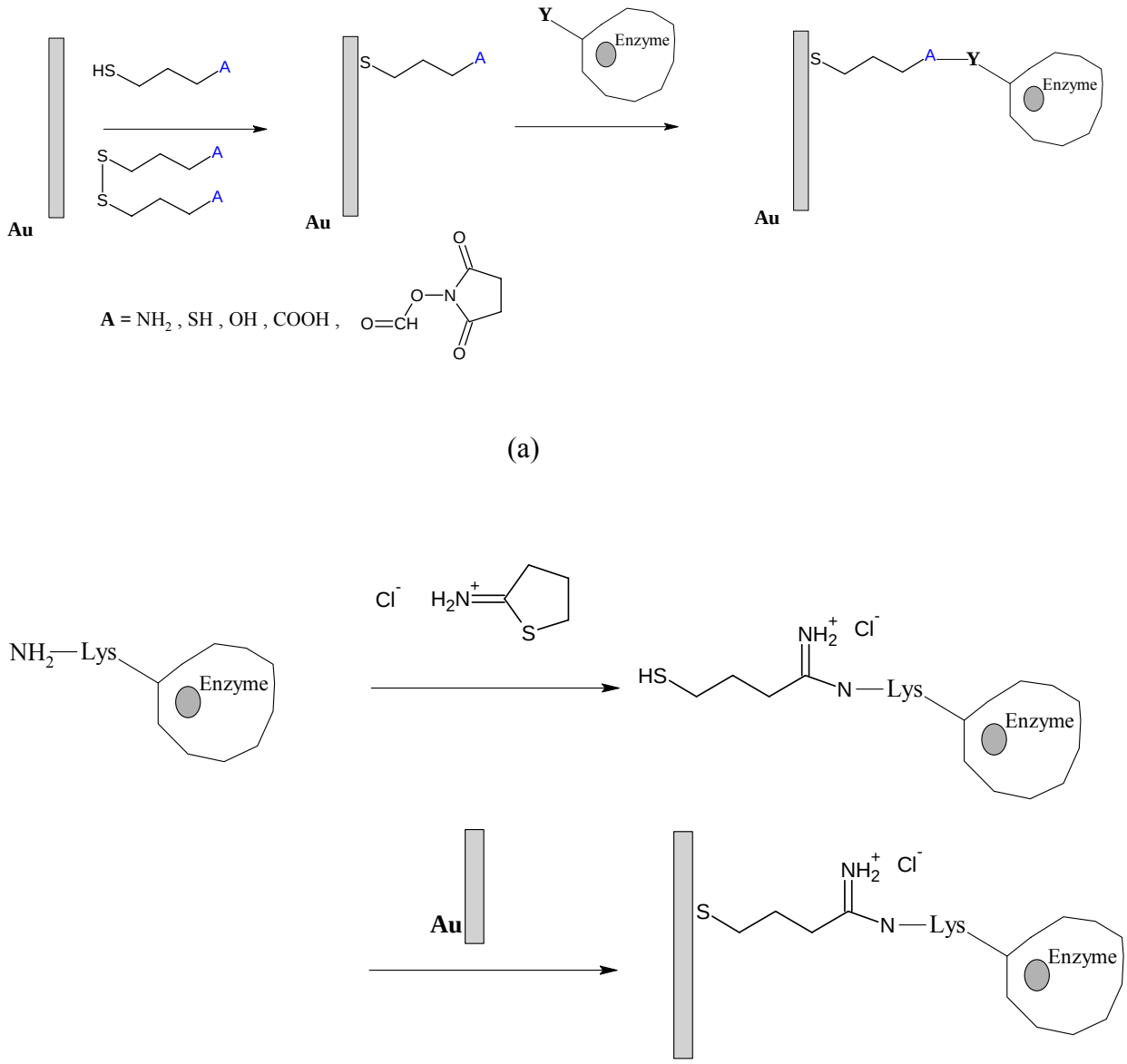

Figure 1.8. Sequential attachment of layers on to a gold electrode .(a) The electrode is functionalized by a self assembled monolayer before attaching the enzyme.(b) A carbon chain with a thiol group is attached to the protein before assembling on to the gold [36].

It is reported that the malate dehydrogenase enzyme-electrode prepared by redox active monolayer assembly rendered a surface coverage of 1.2 x10^{-12} mol cm^{-2} and

exhibited a turnover rate of 190 s^{-1}, whereas the lactate dehydrogenase enzyme-electrode prepared the same way had a surface coverage of 7.0 $x10^{-12}$ mol cm^{-2} and produced a turnover rate of 2.5 s^{-1}. The subsequently conducted chrono amperometric studies has revealed that the NAD^+ cofactor is linked to the PQQ-phenylboronic acid by two different binding modes. The reconstitution of apo-glucose oxidase, on a FAD cofactor linked to a PQQ -phenylboronic acid monolayer assembled on gold electrode has made an electrically contacted enzyme monolayer with surface coverage of 2.1 $x10^{-12}$ mol cm^{-2} exhibiting a turnover rate of 700 s^{-1} at 22 °C [39, 58, 81, 85].The biocatalytic reduction of oxidizers such as oxigen has attracted much less attention compared to the biocatalytic oxidation of fuels. But for a biofuel cell application, it is important to design a functional cathode for the reduction of the oxidizer. Hydrogen peroxide is a strong oxidizer with E° = 1.535V vs. SCE. However, its electrochemical reduction proceeds with a very high overpotential which is less favorable for cathode potential.

The bio-electro catalyzed reduction of H_2O_2 has been accomplished in the presence of various peroxidases (e.g., horseradish peroxidase, Microperoxidase-11 (MP-11,). The MP-11 is reported to have used widely. It is an oligopeptide consisting of 11 amino acids and a covalently linked Fe(III)-protoporphyrin IX heme site. MP-11 posses many advantages over usual peroxidases. It has a much smaller size, high stability and exhibits direct electrical communication with electrodes. It is reported that MP-11 was covalently linked to a cystamine monolayer self-assembled on a Au-electrode. The MP-11 structure suggests the possibility of two different modes of coupling of the oligopeptide to the primary cystamine monolayer: (i) by linking through the carboxylic functions associated with the protoporphyrin IX ligand to the monolayer interface and

(ii) coupling of carboxylic acid residues of the oligopeptide to the cystamine residues. These two binding modes shows similar formal potentials $E^{\circ} = -0.40$V vs. SCE. The interfacial electron transfer rates to the heme sites linked to the electrode by the two binding modes are 8.5 and 16 s^{-1}. Coulometric analysis of the MP-11 redox wave indicates a surface coverage of 2×10^{-10} mol cm^{-2} [85].

The direct electrochemical reduction of oxygen takes place with very large overpotentials (e.g., −0.3Vvs. SCE at a bare Au electrode, pH 7). Thus, catalysts are required in order to utilize oxygen reduction in fuel cells. Inhibiting formation of peroxide or superoxide is a major challenge for the future development of biofuel cell elements because such reactive intermediates would degrade the biocatalysts in the system. The electrodes coated with enzymes and their respective electron transfer mediators (e.g., bilirubin oxidase, or fungal laccase, with 2,2_-azino-bis-(3-ethylbenzothiazoline-6-sulfonate as a mediator) are able to catalyze the reduction of O_2 to H_2O effectively at 0.4 V (vs. SCE), by significantly decreasing the overpotential [46, 47, 57]. The enzymes assembled in layers are much more promising for their use in biocatalytic cathodes. Cytochrome *c* (Cyt *c*) that includes a single thiol group at the 102-cysteine-residue was assembled by Katz and his group as a monolayer on a Au-electrode by covalent linkage of the thiol group to a monolayer-modified electrode. Further, it has been reported that the wild-type Cyt *c* (from *Saccharomyces cerevisiae*) and its mutants (V33C, Q21C, R18C, G1C, K9C and K4C) has been reported to have exhibited direct electrical communication with an Au-electrode [38, 86]. The cyclic voltametry study of the electrode indicated that the resulting heme–protein exhibited direct electrical contact with the electrode. Coulometric study of the electrode indicated a protein coverage of 8 ×

10^{-12} mol cm^{-2}. It has been shown that when the diameter of Cyt *c* which is around 4.5nm is taken into account the surface coverage corresponded to a densely packed monolayer [86].

Entrapment of biocatalyst in a polymer network

Conducting polymers has gained significant interest in the recent past in the area of biosensors. Since the fuel cell is just a composition of two biosensors acting as anode and cathode, much of the work can comfortably be adopted to the fuel cell research. The electrically conducting polymers are known to posses numerous features which allows them to act as excellent materials for immobilization of biomaterials such as enzymes, antibodies, liposomes, and organelles.

The large number of organic compounds which has the property of transferring electrons through its chain can be broadly divided into following categories: (i) charge transfer complexes (ii) organometalic species (iii) conjugated organic polymers. The conducting polymers are different from all the familiar inorganic materials such as semiconductors due to two properties: 1.) the polymers are molecular in nature and 2.) they lack long range order [87]. A key requirement for a polymer to be electrically conducting is that there should be an overlap of molecular orbitals to allow the formation of delocalized molecular wave function. In addition, the molecular orbitals should be partially filled so that there is free movement of electrons. Conducting polymer contains π – electron orbitals which is responsible for their unusual electronic properties such as electrical conductivity, low ionization potential, and high electron affinity. The values of

electrical conductivity obtained for some of those organic polymers were significantly high that they can be approximated as synthetic metals [88].

In a polymer structure, the redox complexes poses a restriction to its mobility in the translational direction but allows electron mobility with adjacent centers [89-91].Redox complexes based on osmium / ruthenium has been tested where it has been immobilized in water soluble polymers such as poly(vinyl imidazole) or poly(allylamine). The redox complexes thus immobilized can further be immobilized on surfaces. Numerous surface immobilization techniques have been discussed in literature and these include: (i) Langmuir-Blogett film [92] (ii) chemicall cross linking [93, 94] and (iii) hydrogels [95]. The enzyme and the redox polymer unit should be linked together in order to facilitate proper electron transfer. This phase separation is overcome by combining the enzyme which is negatively charged and polymer which are positively charged. A study that used a conductive polymer to immobilize glucose oxidase from *Asperigillus niger* in the anode and bilirubin oxidase from *Trechyderma tsunodae* in the cathode has produced interesting results [56]. As the anode redox polymer they used $[Os(N,N'\text{-dialkylated-}2,2'\text{-bis-imidazole})_3]^{2+/3+}$ complex which has a redox potential of -0.19V vs Ag/AgCl. The cathode comprised of polyacrylamide polymer and poly(N-vinylimidazole) complexed with $[Os(4,4'\text{-dicholoro-}2,2'\text{-bipyridyne})_2Cl]^{1+/2+}$ with a redox potential of +0.36V vs Ag/AgCl. The electron transport kinetics in the hydrogel formed upon cross-linking and hydration of the anodic polymer is said to be very fast. [56].

As another example, a biofuel cell developed with poly(aniline)-poly(anion) can be stated. The enzyme lactate dehydrogenase modified with a poly histidine tag has been

immobilized onto poly(aniline)(PANi)- poly(anion) film. Poly(anion) films that was used are poly(vinylsulfonate)(PVS) and poly(acrylate)(PAA). The poly(aniline) doped with PVS/PAA catalyzed the oxidation of NADH at pH 7.0. and the electrode thus constructed oxidized lactate at 0.05-0.1V [96]. Attempts have been made to co-immobilize lactate oxidase and lactate dehydrogenase on conducting polymer films. It has been reported that these composite electrodes have been sensitive to low lactate concentrations such as $5x10^{-5}$ M compared to other electrodes with the single enzyme [97].

A nanostructured electrode for enzymatic biofuel cell based on enzyme encapsulation is also reported . Enzyme encapsulation method despite it restriction to the electron diffusion can make the enzyme more stable. The sol-gel silica matrices and incorporated carbon nanotubes within the matrix facilitate fast electron conduction. The silica matrix brings a sufficient degree of porosity to facilitate the diffusion of both glucose and oxygen to the enzyme. The silica also act as a protective cage for immobilized biomolecules without affecting biological function. This biofuel cell designed on silica sol-gel/carbon nanotube composite electrodes is reported to have generated ~120 $\mu W/cm^2$ at 0.24 V under normal conditions [98].

Hypothesis

Our study of biological fuel cell progressed in two stages. In the first stage we hypothesized that for a yeast based fuel cell run with glucose as the fuel would have better performance in terms of power density, voltage efficiency, open circuit voltage and internal resistance in the presence of mediators. Methylene blue in the anode and the potassium ferricyanide in the cathode would constitute an effective mediator couple. In

the second stage of the experiment we focused to gain more specificity on the substrate by using an enzyme rather than microorganisms. In the second stage we hypothesized that a gold electrode coated with lactate dehydrogenase coupled with a Pt electrode would make up a workable fuel cell using lactate as the fuel.

CHAPTER II

MICROBIAL FUEL CELL

Chapter Summary

Saccharomyces cerevisiae, the fungal strain present in common Baker's yeast was used in a microbial fuel cell in which glucose was used as the carbon source. Methylene blue was used as the electronophore in the anode compartment whereas ferricyanide and the methylene blue were tested as electron acceptors in the cathode compartment. Microbes in a mediator-free environment were used as the control. The experiment was performed in both open and closed circuit configurations under different loads ranging from 100KΩ to 400Ω. The eukaryotic S. Cerevisiae based fuel cell showed improved performances when methylene blue and ferricyanide were used as electron mediators with a maximum power generation of 146.71±7.7mW/m^3 when compared with a mediator-less control. The fuel cell generated a maximum open circuit voltage of 383.6±1.5 mV and recorded a maximum efficiency of 28±1.8 % at 100KΩ external load.

Introduction

Due to increasing energy prices and concerns on long-term energy security, there is a renewed interest on bio-renewable energy generation. Hence, direct electricity generation from glucose, a bio-renewable feedstock, has regained momentum. This study is an in-depth look at the behavior of a fuel cell using Baker's yeast (*Saccharomyces*

cerevisiae) in a proton exchange membrane (PEM) microbial fuel cell (MFC). Yeast based fuel cells are of interest since these could be easily retrofitted into ethanol plants for in situ power generation. The function of microbes in a fuel cell is to catalyze the reaction that involves conversion of chemical energy into electrical energy [28, 43]. The metabolic processes of these microorganisms produce electrons by oxidizing the carbon source, which in many applications, is a carbohydrate monomer. The electrons generated at the anode can then be passed through an external circuit to produce power. These electrons enter the cathode to combine with the protons (H^+) that transfer through a Proton Exchange Membrane (PEM) and binds with externally provided oxygen to form water. Presently, Microbial Fuel Cell (MFC) research is highly focused on wastewater treatment. The organic sludge is used as the carbon source for organisms to oxidize. To date, different organisms have been experimented with in MFCs, and depending on the need for presence or absence of mediators to complete the redox mechanism, two main types of fuel cells have been documented: (1) Fuel cells with mediated electron transfer and (2) Fuel cells with direct electron transfer [99].

In fuel cells with mediated electron transfer, an intermediate molecule, preferably a dye, will shuttle the electrons between microbes and the electrode. The staining ability of a dye helps it to stick to the cellular membrane and help transfer electrons and protons. Direct electron transfer is now of research interest where the organisms generate their own mediators, making exogenous mediators unnecessary. Indigenous mediators reduce the risk of poisoning the medium, which is considered a serious drawback of the exogenous mediators. Commonly used organisms in direct electron transfer fuel cells are *Shewanella putrefaciens, Geobacter sulfurreducens, Geobacter metallireducens* and

Rhodoferax ferrireducens [100-102]. Tests with these organisms have proved higher coulombic efficiencies, which translates to high electron transfer rates between the species and the electrode. However, the coulombic efficiency itself is inadequate to determine the fuel cell behavior as it does not sufficiently explain the energy generation mechanism/s in the cell. Therefore, additional parameters such as: (1) Metabolism rate of the microbial species, (2) Electron transfer rate of the microorganisms, (3) The effectiveness of the proton exchange membrane, (4) Efficiency of the cathode reaction and (5) Internal resistance have to be considered for effective performance analysis of a fuel cell. This work, in part, attempts fulfilling this knowledge gap using *Saccharomyces cerevisiae* as the model microorganism. There is little to no documented research on using yeast, a harmless microorganism, in a fuel cell setting. This study is an in-depth look at the behavior of a fuel cell using Baker's yeast (*Saccharomyces cerevisiae*) in a proton exchange membrane microbial fuel cell. Yeast based fuel cells are of interest since these could be easily retrofitted into ethanol plants for in situ power generation.

The metabolism of yeast is well understood. Depending on the availability of oxygen, the glucose metabolism takes two distinct pathways: (1) Anabolic pathway which leads to production of new cellular materials and (2) Catabolic pathway which removes electrons from substrates or intermediates to generate energy where NADP or NAD is used as cofactors. In yeast, the major source of energy is glucose and the principle catabolic pathway is glycolysis where glucose is converted to pyruvate. To continue energy production, pyruvate will undergo further breakdown under two processes i.e.: "respiration" and "fermentation". Aerobic respiration of eukaryotes is different to anaerobic fermentation as shown in Figure 2.1. In aerobic respiration, the

metabolic intermediates of the glycolysis process enter the citric acid cycle in the mitochondria whereas in anaerobic fermentation, the conversion gets completed within the cytoplasm without the interference of an organelle. In order to keep the glycolysis reaction continuous, the NADH is recycled back to NAD^+ by alcohol dehydrogenase present in the cytoplasm[103]. Anaerobic conditions are desirable for a fuel cell because oxygen, the terminal electron acceptor in the cathode, may impede the fuel cell function if present in the anode compartment. *S. Cerevisiae* is a facultative anaerobic organism and therefore, it can thrive in both aerobic and anaerobic conditions. Under aerobic fermentation, *S. Cerevisiae* undergoes cell growth while under anaerobic conditions the organism enters into a catabolic pathway in which ethanol is produced as the final product as depicted in Figure 2.1 [103, 104].

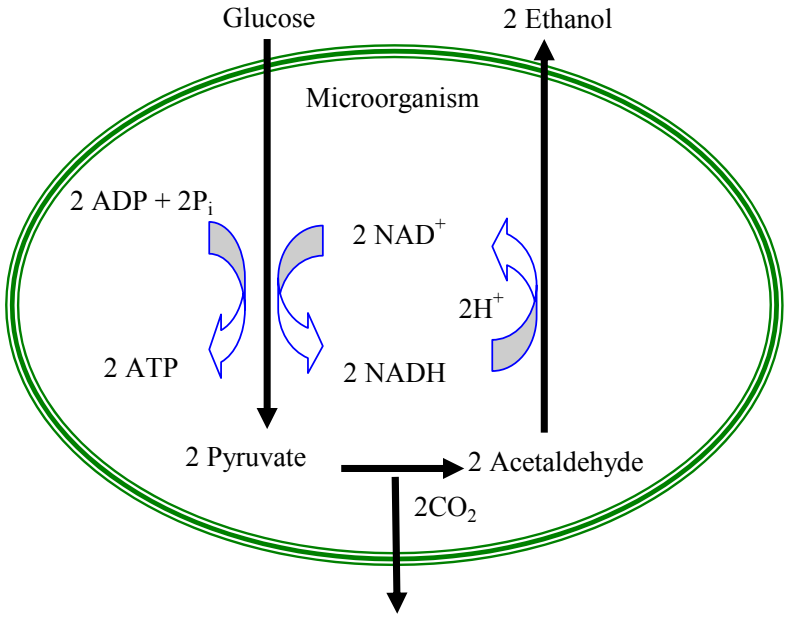

Figure 2.1. Anaerobic fermentation pathway of *Saccharomyces cerevisiae* -under anaerobic conditions [109].

In a complete oxidation of the fuel glucose, it undergoes a reaction as given in Equation 2.1, while its electrons are taken up by a mediator molecule which will shuttle electrons from micro organism to the anode [99]. In the absence of oxygen in the anode, the electrons can be diverted to the electrode and made to pass through an external circuit, ultimately to combine with an electron acceptor, namely, molecular oxygen as given in Equation 2.2 [99]. The *Saccharomyces cerevisiae* based fuel cell was developed based on the above principle. One of the main reasons behind selecting this organism for further study was the non-immunologic nature of Baker's yeast and the possibility of incorporating the fuel cell to an ethanol producing bio reactor.

$$C_6H_{12}O_6 + 6H_2O \longrightarrow 6CO_2 + 24H^+ + 24e^- \qquad E^0 = 0.014V \quad (2.1)$$

$$6O_2 + 24H^+ + 24e^- \longrightarrow 12H_2O \qquad E^0 = 1.23V \quad (2.2)$$

Objectives:

The main objective of this study is to parameterize the performance of a *Saccharomyces cerevisiae* based fuel cell. The effect of extraneous mediators on open circuit voltage, current and power under different loads, the internal resistance and the efficiency were determined.

Materials and Method

Construction of the fuel cell.

The fuel cell chamber was constructed from PVC as shown in Figure 2.2. The internal diameter of the chambers was 5 cm and each compartment had a volume of 500ml. The two chambers were separated by a Proton Exchange Membrane (PEM) where the membrane was held by a coupling between the chambers as shown in Figure 2.2. A DuPont Nafion 117 PEM was purchased from the Iron Power Co. and each experiment was performed with a new membrane to avoid any interferences and/or contaminations from previous experiments. The electrodes were 45 PPI (Pores per Inch) Reticulated Vitreous (RV) carbon, with dimensions 1"x 1" x 6" purchased from ERG (Oakland CA). Copper (Cu) wires were soldered to the electrodes by using a conductive epoxy. A digital pH transmitter (Sensorex, PHMA transmitter and pH probe) was used to measure pH variations during experimentation. The IoTech WaveBook 12 with a sampling rate of 0.1Hz was used as the automated data acquisition system.

Operation of the Fuel cell.

Cell growth measurements were not observed in order to minimize oxygen contamination to the fuel cell as well as to keep liquid volumes in the anode compartment static during experiments. On each operation, the fuel cell compartments were cleaned and the electrodes were autoclaved for 30 min. All the substrates, i.e., *Saccharomyces cerevisiae* , methylene blue (MB), potassium ferricyanide (PF) and D-glucose were purchased from Sigma Aldrich. The concentration of both MB and PF solutions were 50mM.

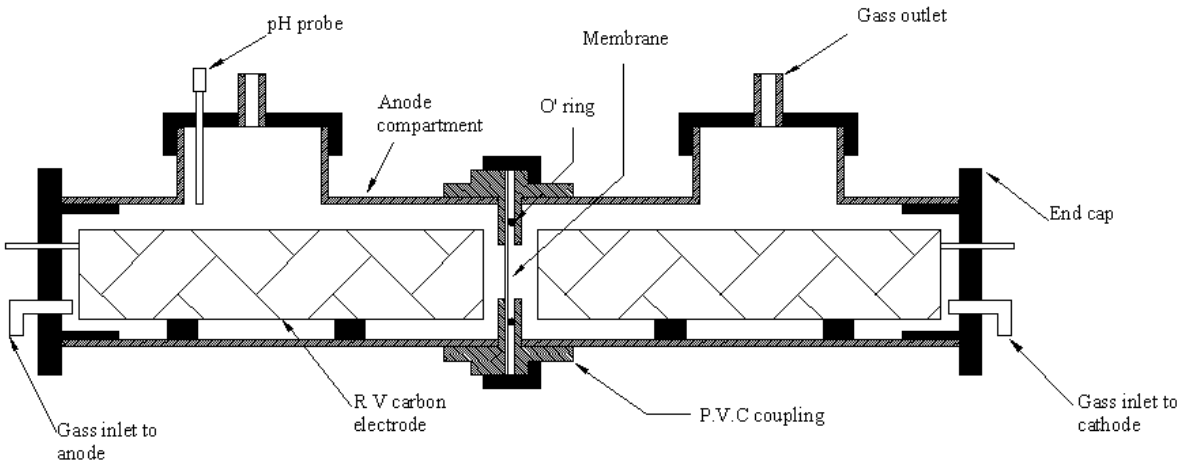

(a)

(b)

Figure 2.2. The sectional view and the actual setup of the fuel cell (a) The sectional view of the fuel cell. (b) Actual view of the fuel cell.

The anode solution was prepared with 2g of yeast and 0.12M D-glucose was prepared in either MB or de-ionized water — stirred well using a magnetic stirrer. In the experiment, the combinations of the solutions were selected according to Table 2.1. After a new batch was fed, both anode and cathode compartments were sparged with 300ml/min CO_2 and O_2 respectively. The open circuit voltage (OCV) was measured continuously using the automated data acquisition system and averaged when the

readings are stable. A completely randomized designed was used in the experiment and the data were analyzed using statistical analytical software SAS. All the inferences were based at P = 0.05 significant level. The data points and the values are represented with ± standard error.

Table 2.1. The experimental Design

Exp. Number	Organism	Substrate	Mediator- (anode)	Catholyte
EX1	Yeast	Glucose	Methylene blue	Methylene blue
EX2	Yeast	Glucose	Methylene blue	$K_3Fe(CN)_6$
EX3	Yeast	Glucose	Methylene blue	Water
EX4	Yeast	Glucose	Water	Water
EX5	Yeast	Glucose	Water	Methylene blue
EX6	Yeast	Glucose	Water	$K_3Fe(CN)_6$

Results and Discussion

Performance under no load conditions.

During the first phase of the experiment, a cyclic voltametry (CV) study was conducted to understand the electron transfer kinetics of the MB and PF. Since the MB is used as the mediator in the anode, it is necessary for the mediator to be reversible between the reduced and the oxidized states.

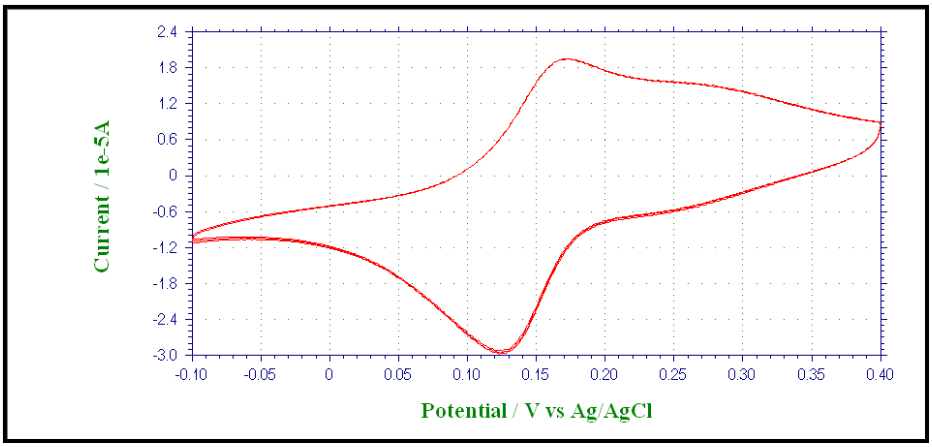

Figure 2.3. The cyclic voltammogram for 50mM methylene blue solution. Scan rate 0.05V/s , potential range -0.1V- 0.4V.

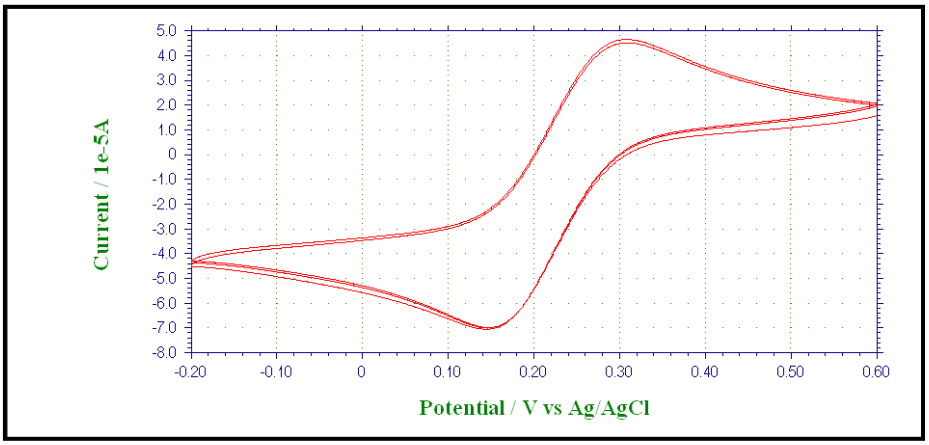

Figure 2.4. The cyclic voltammogram for 50mM potassium ferricyanide solution. Scan rate 0.05V/s and the potential range -0.2V to 0.6V.

Studying the Figure 2.3 it can be explained that MB is reversible between its reduced (Methylene Blue) and the oxidized (Methylene White) states as the peak potential difference is very close to 59mv. The CV study for the PF as given in the Figure 2.4 indicates a quasi-reversible behavior between its reduced and the oxidized states. In the microbial fuel cell, glucose oxidation is the main source of energy generation. The

individual potential of both anode and cathode depends on the redox potential of the reactions at the electrode. The half reaction of the oxidation of glucose Equation 2.1 is having a standard potential of 0.014V, and theoretically, will determine the anode potential. However, it should be noted that the energy generated will not be available to extract directly at the electrode - since this conversion takes place in a microbe cell extraneous to the anode. On the other hand, the half reaction of the cathode, which is the reduction of molecular oxygen Equation 2.2 will determine the potential of the cathode. The difference between the Equation 2.1 & 2.2 will give the fuel cell its theoretical maximum of 1.216V. When the reaction of Equation 2.1 takes place inside the microorganism, the electrons it generate should be transferred to the anode. The natural mediator inside the organism is NAD and this initiates a redox couple NAD^+ / NADH as given in Equation 2.3 inside the cell of the organism, where on the periphery of the anode, the electrons will be discharged [99]. Due to the cellular membrane, the electron transfer to the electrode is hindered and the electrode potential will depend on the redox potential of the NAD^+ / NADH couple.

$$NAD^+ + H^+ + 2e \longrightarrow NADH \qquad E^0 = 0.01V \quad (2.3)$$

$$\text{Methylene Blue}_{\text{reduced}} \longrightarrow \text{Methylene Blue}_{\text{oxidized}} + e \qquad E^0 = -0.021V \quad (2.4)$$

The oxidation of the NADH is slow and inefficient. In the case of yeast, NAD^+ / NADH redox couple would determine the anode potential if no electron shuttling mediator was available. The use of MB as an intermediate molecule will be effective in

this regard as it will get reduced relatively easily and it undergoes a reversible reaction. In the presence of a mediator molecule, the potential of the anode will be determined by the potential of the oxidation reaction as given in Equation 2.4. In the six experiments conducted, the reactions at the anode and the cathode compartments are represented in the Table 2.2. At the cathode, the reduction of oxygen molecule takes place with a high over potential when there is no electron transfer molecule is present. However, $Fe(CN)_6^{4-}$ / oxygen coupled reaction and the MB/oxygen coupled reaction reduces the over potential and make it easier for molecular oxygen to get reduced. At the cathode, when MB / $Fe(CN)_6^{4-}$ is present, the potential is determined by the redox reaction depicted in Equation 2.4 / Equation 2.5.

$$Fe(CN)_6^{3-} + e^- \longrightarrow Fe(CN)_6^{4-} \qquad E^0 = 0.424V \quad (2.5)$$

Figure 2.5.B represents the anode potential converted to the normal hydrogen electrode (NHE) potential values. The potential changed from positive to more negative with time, indicating that the anode oxidation reaction dominated. According to Figure 2.5.B, out of all experimental units, EX1 (MB(ac)/MB(cc)) exhibited the highest anode potential of 0.394±0.017V. All the samples with MB in the anode compartment exhibited higher potentials, indicating that MB functioned as a superior mediator.

When the anode compartment had no mediators the EX5 (water(ac)/MB(cc)) gave the lowest potential of 0.096±0.007V. On the cathode compartment, the potential values remained positive. It was observed that with time, the positive values increased implying that the redox reaction became dominant. Of all the experimental units, EX2

(MB(ac)/PF(cc)) & EX6 (water(ac)/PF(cc)) gave the highest cathode potentials with 0.578±0.002 and 0.581±0.001V respectively Figure 2.5.C.

Table 2.2. Fuel cell reactions for different experiments: (a) the reactions in the anode compartment and (b) the reactions in the cathode compartment.

(a)

Experiment	Reactions in the anode compartment
EX1	$MB_{(oxidized)}+NADH_{(yeast)} \longrightarrow NAD^{+}_{(yeast)} + MB_{(reduced)}$ $MB_{(reduced)} \longrightarrow MB_{(oxidized)} + e^{-} + H^{+}$
EX2	$MB_{(oxidized)}+NADH_{(yeast)} \longrightarrow NAD^{+}_{(yeast)} + MB_{(reduced)}$ $MB_{(reduced)} \longrightarrow MB_{(oxidized)} + e^{-} + H^{+}$
EX3	$MB_{(oxidized)}+NADH_{(yeast)} \longrightarrow NAD^{+}_{(yeast)} + MB_{(reduced)}$ $MB_{(reduced)} \longrightarrow MB_{(oxidized)} + e^{-} + H^{+}$
EX4	$NADH_{(yeast)} \longrightarrow NAD^{+}_{(yeast)} + H^{+} + e^{-}$
EX5	$NADH_{(yeast)} \longrightarrow NAD^{+}_{(yeast)} + H^{+} + e^{-}$
EX6	$NADH_{(yeast)} \longrightarrow NAD^{+}_{(yeast)} + H^{+} + e^{-}$

(b)

Experiment	Reactions in the cathode compartment
EX1	$4MB_{(oxidized)}+ 4H^{+} + 4e^{-} \longrightarrow 4MB_{(reduced)}$ $4MB_{(reduced)} + O_2 \longrightarrow 2H_2O + 4MB_{(oxidized)}$
EX2	$4PF_{(oxidized)} + 4e^{-} \longrightarrow 4PF_{(reduced)}$ $4PF_{(reduced)} + O_2 + 4H^{+} \longrightarrow 2H_2O + 4PF_{(oxidized)}$
EX3	$4H^{+} + O_2 + 4e^{-} \longrightarrow 2H_2O$
EX4	$4H^{+} + O_2 + 4e^{-} \longrightarrow 2H_2O$
EX5	$4MB_{(oxidized)}+ 4H^{+} + 4e^{-} \longrightarrow 4MB_{(reduced)}$ $4MB_{(reduced)} + O_2 \longrightarrow 2H_2O + 4MB_{(oxidized)}$
EX6	$4PF_{(oxidized)} + 4e^{-} \longrightarrow 4PF_{(reduced)}$ $4PF_{(reduced)} + O_2 + 4H^{+} \longrightarrow 2H_2O + 4PF_{(oxidized)}$

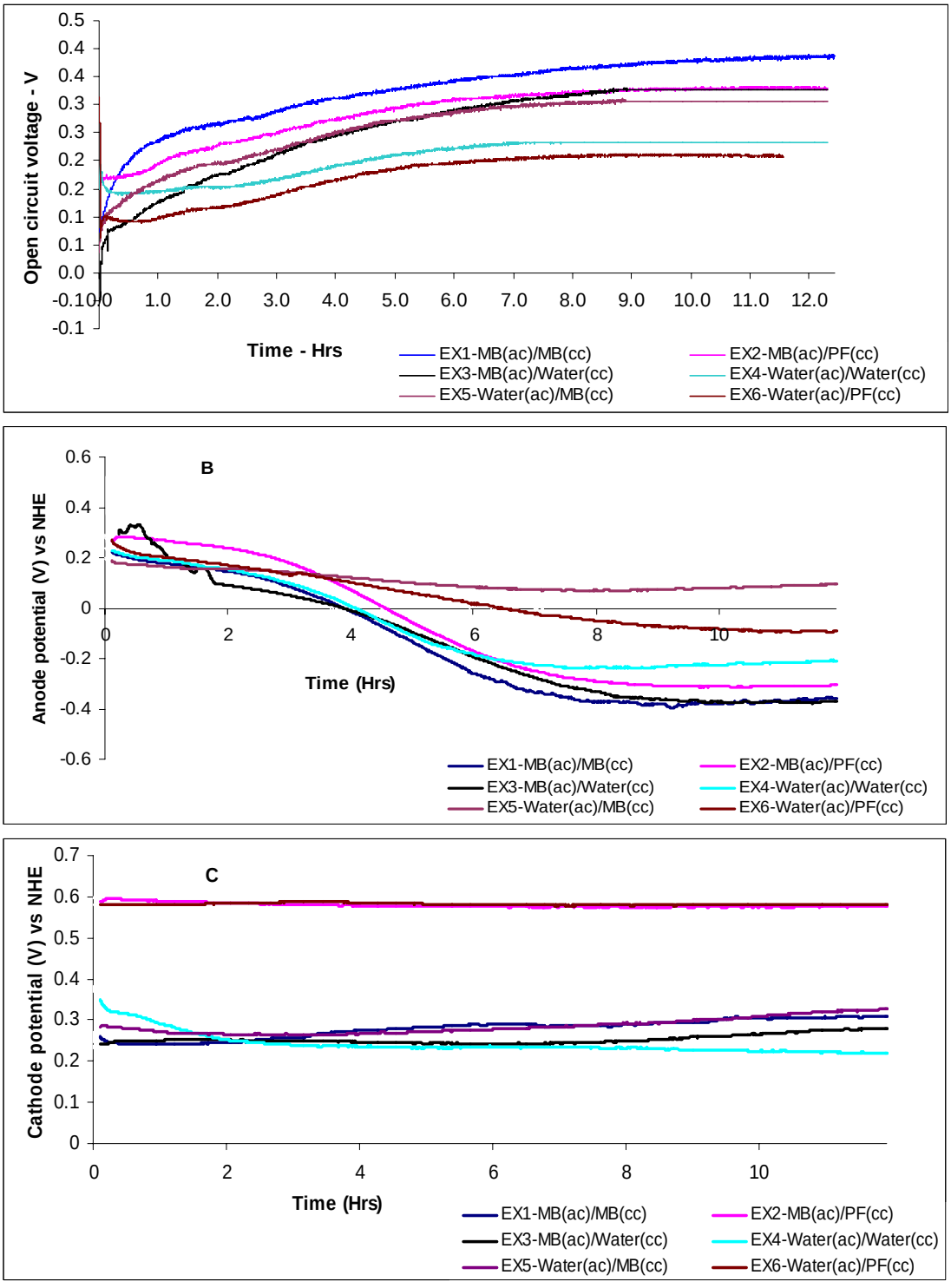

Figure 2.5. Potential measurements of the cell (A). the open circuit voltage between anode and the cathode; (B).the potential variation in the anode; (C). the potential variation in the cathode.

In both these cases, the cathode solution was $K_3Fe(CN)_6$. However, a relatively higher potential was recorded for EX6 (water(ac)/PF(cc)). This indicated that the electrolyte of the opposite compartment had a significant effect on the potential of a particular electrode. For example, the anode potential of EX1 (MB(ac)/MB(cc)) and EX2 (MB(ac)/PF(cc)) were not the same even though the EX1 and EX2 anode solutions were similar. This is because the cathode solutions of the two experimental units were different. Similarly, the cathode potential of EX2 (MB(ac)/PF(cc)) and EX6 (water(ac)/PF(cc)) were not the same even though the cathode solutions of EX2 (MB(ac)/PF(cc)) and EX6 (water(ac)/PF(cc)) were similar. This behavior could be attributed to the differences of the anode solutions in the two experimental units.

Another notable observation was migration of mediators across compartments - though at a relatively slower rate (as indicated by slow coloration of the opposite compartment when methyl blue was used in one compartment). This purports that even though the cell is compartmentalized, the membrane separating the chambers were not totally impermeable for the mediator molecules. The implication of this cross over is reduction of possible maximum voltage differences which in turn reduce the power capacity of the fuel cell.

Figure 2.5.(A) shows the results that were obtained by direct measurement of the potential difference between the electrodes. It was evident that the direct measurement results were different from the values obtained by taking the difference of the individual anode and the cathode potentials. The possible explanation for this is the existence of a potential difference between the interfacing liquids in the cathode and anode compartments.

Performance under load conditions.

The vitreous carbon electrode of 45.PPI imparts a large surface area exposed to the solution. Therefore, parameters like current and power was presented with respect to the electrode volume rather than the electrode surface area in the cell performance analysis. For testing the fuel cell under different loads, the cell was connected to a decade resistor box and the potential difference across the load was recorded. The cell was laden under three load ranges, A, B and C as given in Table 2.3, where each instance, the cell was loaded with an external resistor for 10 minutes. When loading the cell in the 100,000 – 10,000Ω range, the potential drop was almost negligible. However, it was observed that as the load decreased, the current increased resulting in more losses. The effect of mediators used in the cathode is elucidated in Figure 2.6(iii). The experimental pairs EX2 (MB(ac)/PF(cc)) & EX6 (Water(ac)/PF(cc)), EX1 (MB(ac)/MB(cc)) & EX5 (Water(ac)/MB(cc)), EX3 (MB(ac)/Water(cc)) & EX4 (Water(ac)/Water(cc)) had identical cathode solutions. The behavior of voltage and current of each pair shows a significant similarity (see Figure 2.6 (ii)-2.6 (iii)) and it bears the proof that the cathode solution has a significant effect on the fuel cell parameters.

Table 2.3 The loading patterns for the cell.

Loading pattern	**Range**	**Increment**
A	400Ω – 1000Ω	100Ω
B	1KΩ – 10KΩ	1KΩ
C	10KΩ – 100KΩ	10KΩ

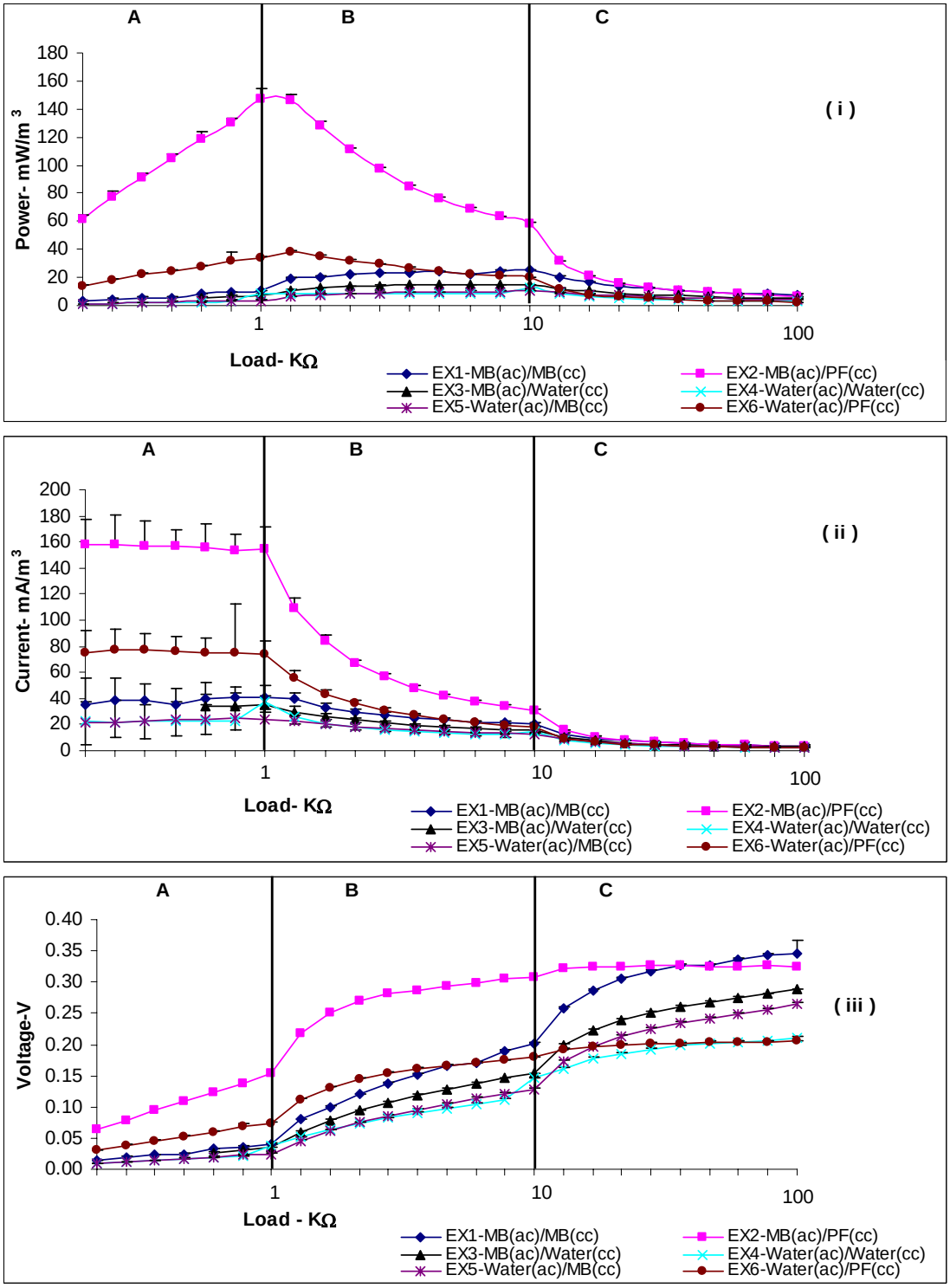

Figure 2.6. Variation of fuel cell parameters under different load conditions (i.) Power Vs Load, (ii.) Load current Vs Load and, (iii.) Load voltage Vs Load. The error was represented as (± standard error).

In Figure 2.6 (i), the EX2 (MB(ac)/PF(cc)) showed the best performance in terms of power generation where 146.71±7.7mW/m^3 was measured at the load of 1000Ω. The internal impedance of the fuel cell has a significant effect in determining the voltage output. Impedance rather than the resistance is quite appropriate for a BFC as the cell has a capacitive component between the two electrodes [105]. The fuel cell schematically can be represented with the internal impedance component R_i, as shown in Figure 2.7. The impedance values for EX2 (MB(ac)/PF(cc)) and EX6 (Water(ac)/PF(cc)) were the lowest and were fairly stable over a wider range of loads as shown in Figure 2.8. All the other experimental units showed relatively higher impedance values varying significantly with the cell loading range. Since the electrodes used in the experiment were fairly large, it could be anticipated that the capacitive component is significantly large [105].

It was observed that the internal impedance was substantially influenced by the cathode solution. Presence of $K_3Fe(CN)_6$ in the cathode significantly reduced the internal impedance. This may be attributed to the presence and increased mobility of ions in the solution. On the other hand, experimental units containing MB in the catholite caused higher resistance values explaining further that cathode solutions should be ionic in order to lower the impedance. The lowest impedance recorded was approximately 454±26.8 Ω as per Figure 2.8 and it was obtained when the cell was loaded with 20KΩ in EX2 (MB(ac)/PF(cc)). A current of 16.09±8 μA was recorded when the cell was operating under lowest impedance. It should be noted that in addition to the solution properties, the membrane and gap between the electrodes also made significant contributions to the internal impedance.

$$R_i = \frac{[\xi - V_e]}{V_e} \times R_e$$

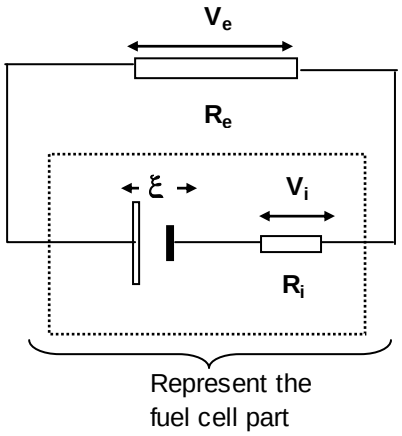

Figure 2.7. A model diagram for a fuel cell. (R_i the internal impedance , ξ the OCV of the cell, and R_e the external load V_e and V_i are the voltage drops across R_e and R_i)

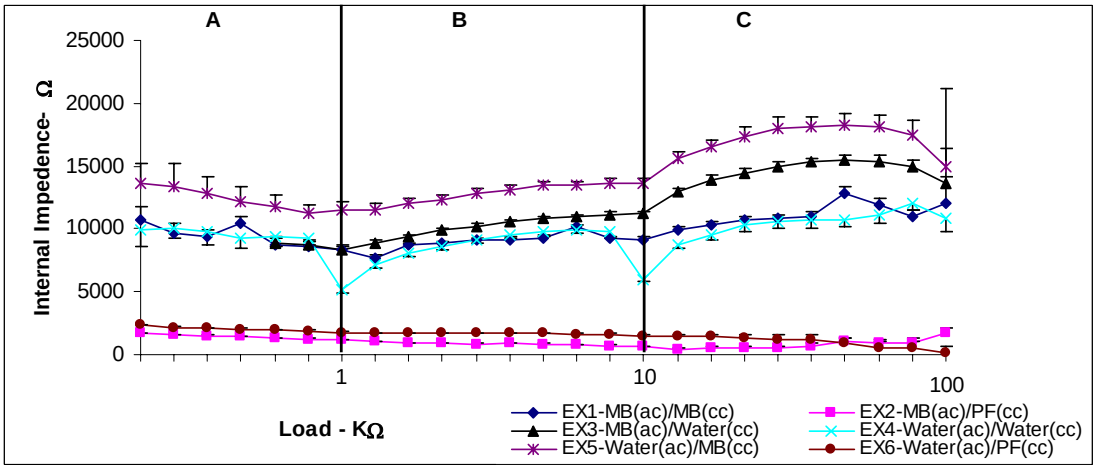

Figure 2.8. The fuel cell internal impedance variation under different loads

Fuel Cell Efficiency

The chemical efficiency of the fuel cell over the load range tested is dependant on the type of reaction the fuel (glucose) undergoes. Thermochemical efficiency (μ_{th}) of

glucose metabolism could be calculated according to Equation 2.6 where ΔG_f - Gibbs free energy, ΔH – Enthalpy of formation of glucose. For glucose, ΔG_f = -910KJ/mol , ΔH = -1268KJ/mol and according to Equation 2.6, the efficiency of conversion is 0.718. Accordingly, from its formation enthalpy, 71.8% of energy is available for use.

$$\mu_{th} = \Delta G_f / \Delta H \qquad (2.6)$$

.
The operational efficiency of a fuel cell is an important parameter. The Electrical Efficiency (μ) of the fuel cell is given by the Equation 2.7 where ΔV is the voltage across the load , ΔH is the calorific value of Glucose, n - is the number of electron moles transferred across the load and F- is the Faraday constant [7].

$$\mu = \frac{\Delta V}{\Delta H / n * F} \qquad (2.8)$$

The efficiencies calculated for the six experiments are depicted in Figure 2.9. For higher load conditions or when the load currents were low, the cell showed higher efficiencies. At the best operating point where the maximum power was recorded (1000Ω load), the efficiency for EX2 (MB(ac)/PF(cc)) was 12.6±0.2 %. The highest efficiency obtained from the fuel cell was 28±1.8 % for the EX1 at 100KΩ. However, for EX2 (MB(ac)/PF(cc)), the efficiency value remained at 26.4% for a wide range of external loads. This fairly constant efficiency displayed by EX2 (MB(ac)/PF(cc)) could be attributed to the stable electron transfer between the mediator molecules and the electrode. However, when the current demand increases, with the decrease in external

load, the electron generation and transfer at the anode is inefficient which results in a reduction of the load voltage. Consequently, the efficiency too will drop. In addition to the internal resistance, there is a capacitive effect building up near the electrodes which creates an additional potential drop between the fuel cell electrodes. This effect, known as double layer capacitance, was not intended to be studied in this experiment.

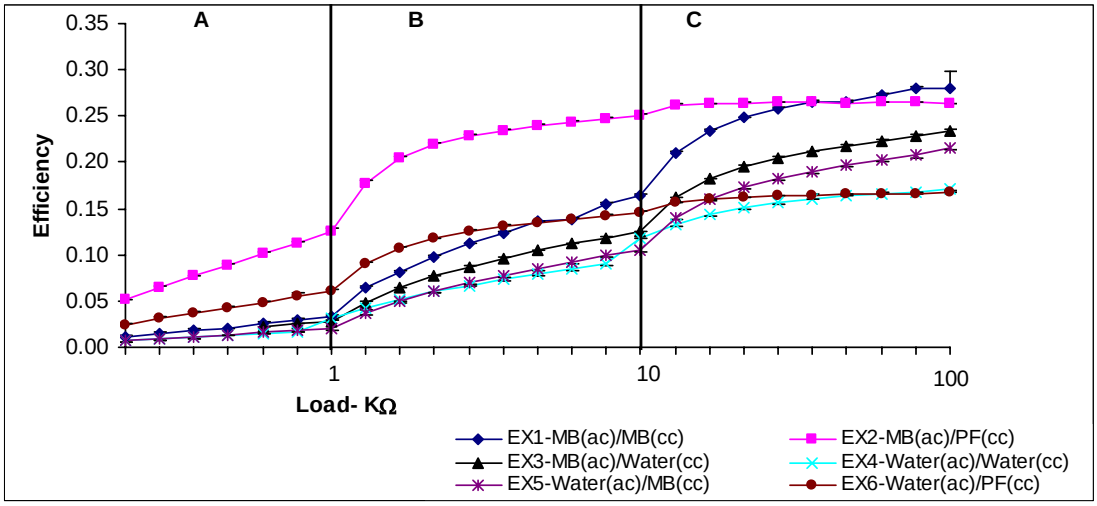

Figure 2.9. The efficiency variation of the fuel cell under varying external loads

Conclusions

Saccharomyces cerevisiae performed favorably as the bio-catalyst in a microbial fuel cell powered by glucose. The relatively low current generation under different loads can be attributed to the slow metabolic rate of yeast, high over potential for oxidation of O_2 at the reticulated vitrious carbon cathode, and electron transfer inefficiencies between the mediator molecule and the microorganism's cell wall. Presence of methylene blue and the ferricyanide electronophores significantly enhanced the fuel cell performance. The

cathode solution showed to be having a great influence on the potential across the cell terminals. The microbial fuel cell generated a maximum power of 146.71±7.7 mW/m^3 with a maximum open circuit voltage of 383.6±1.5 mV. The maximum operational efficiency of the fuel cell was 28±1.8 % which was obtained when methylene blue was the mediator in both anode and cathode compartments.

CHAPTER III

ENZYME BASED FUEL CELL

Chapter Summary

Lactate dehydrogenase (LDH), a NAD dependent oxidoreductase enzyme, was immobilized on a 0.5mm gold wire by layer by layer assembly technique. LDH coated electrode was used as the anode of the fuel cell and a Pt wire of 0.5mm was used as the cathode. The electrodes were assembled in a single chamber fuel cell where lactate solution was used as the fuel substrate. LDH coated anode catalyzed the oxidation of lactate to pyruvate and the Pt helped catalyzing the reduction of oxygen to water. Three parameters were selected to understand the behavior of the fuel cell under different load conditions. The parameters, i.e., lactate concentration, temperature of the cell and the flow rate, were all changed within the physiological ranges to emulate the performance as an implantable fuel cell. The cell reported an average open circuit voltage of 266±1 mV and an efficiency of 3.6±0.25 %.

Introduction

Biological fuel cells has attracted extensive attention in the recent past [99, 106]. The function of the biocatalyst in such biological fuel cells is to catalyze the reaction of the fuel oxidation in order to convert chemical energy to electrical energy [10]. Bio catalysts exist in two forms: either in the microbial form or enzymatic form. The enzymes

are substrate specific catalysts and bear substantial merits over microbes for miniaturized applications in terms of power density and size. Large array of enzymes has been tested for oxidation of substrates such as glucose, lactate, methanol etc.

In mammalian species, L-lactate is constantly produced from pyruvate by LDH according to the reaction scheme given in Figure 3.1 in the process of rigorous muscular work under anaerobic conditions. The produced lactate will be transported to the liver for conversion back to pyruvate by the cori-cycle. The concentration of blood lactate is usually 1-2 mmol/L at rest, but can rise to over 20 mmol/L during intense exercise as shown in Figure 3.2.

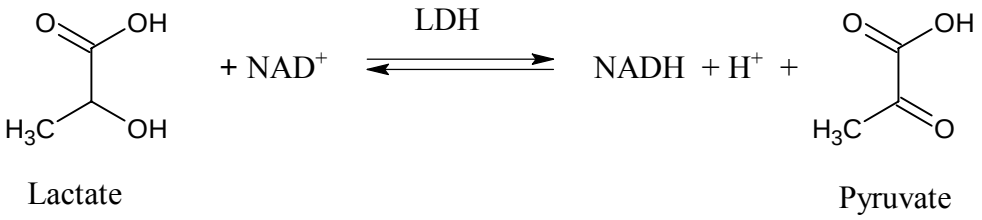

Figure 3.1. Lactate is oxidized to pyruvate in a reversible reaction which is catalyzed by LDH.

Blood lactate can be used as a potential fuel source for a fuel cell that uses LDH in its anode. Among them covalent attachment of the enzyme to a self assembled monolayer has been widely accepted as a highly effective criteria as compared to others. Many methods have been tested for attaching LDH on to an electrode. However, for in vivo applications such composite electrodes has to meet strict standards such as biocompatibility, longevity, and molecular stability. In addition to the electrode

assembling techniques the fuel cell architecture is also an important factor to be considered in constructing a fuel cell.

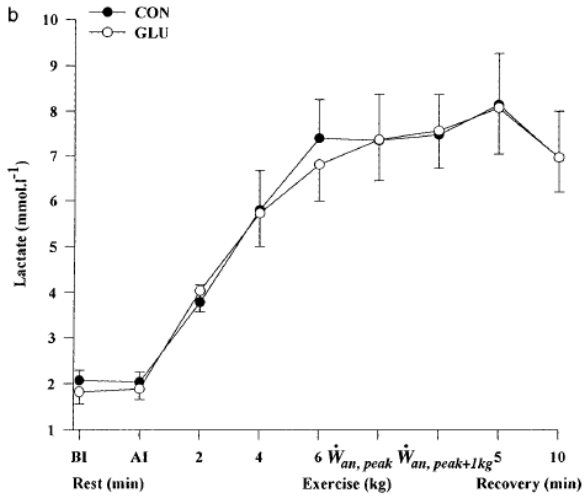

Figure 3.2. Variation of blood lactate before and after exercise on humans. The experiment has been conducted in two environments. Glucose being injected to the patient (GLU) and without glucose (CON) [107].

There are mainly two types of enzymatic fuel cells that have been reported namely: compartmentalized and non compartmentalized fuel cells [46, 58, 108]. Due to enzymes being highly substrate specific, with enzyme/s immobilized on the electrode, it is possible to go for non-compartmentalized fuel cell designs. This is been possible since electron transfer from the co-factor of the enzyme to the electrode is significantly fast [109] and it significantly difficult for the competing oxygen to get reduced by capturing electrons from the active site due to enzyme specificity. On the other hand when the enzyme is diffusional in the fuel cell, the anode and the cathode compartments have to be separated by a proton exchange membrane to inhibit species cross over. The cathode of the fuel cell is designed mainly to reduce oxygen and will undergo the reaction depicted

in Equation 3.1. Pt is a strong catalyst for catalyzing the reduction of oxygen. However, there are enzymes such as bilirubin oxidase , Cytochrome C and laccase that have been successfully used in the cathode for catalyzing the reduction of dioxygen [63, 106].

$$4H^+ + O_2 + 4e \rightleftharpoons 2H_2O \qquad (3.1)$$

A fuel cell as a power source should meet several important requirements to successfully run an external device. These include: (i) A stable voltage out put under load; (ii) Low internal resistance; and (iii) High durability. The power available at the fuel cell terminal, as given by Equation 3.2, is controlled by the load current and the voltage across the load.

$$P = V_{cell} \times I_{cell} \qquad (3.2)$$

(P= cell power , V_{cell} = cell voltage , I_{cell} = cell current)

Objective

It is hypothesized that a gold electrode coated with LDH as the anode and coupled with Pt as the cathode would make a functional fuel cell.

Materials and methods

Construction of the anode was based on layer by layer assembly of molecules by electro static forces. LDH was immobilized on a Au electrode by self assembling four consecutive molecules as described in literature [84]. Subsequent to preliminary studies,

the methods were modified by addition of *N*-hydroxysuccinimide (NHS) with 1-ethyl-3-(3-dimethylaminopropyl)carbodiimide (EDC) to increase the charge transfer characteristics of the electrode. Cystamine , Pyrroloquinoline quinone (PQQ) , Phenyl boronic acid , NAD^+ and Glutaric dialdehyde were purchased from Sigma Aldridge . EDC and NHS were purchased from Pierce and Lactate dehydrogenase (LDH, E.C.1.1.1.27) from rabbit muscle was purchased from Worthington Co. Gold and Pt electrodes were purchased from Goodfellow. Ultra pure Mili-Q water of ~17MΩ was used throughout the experiment. National instrument's CDAQ data logging system was used to record data. CH Instrument's CHI6002 potentiostat was used for cyclic voltametry studies of the electrode. After rigorous cleaning with HNO_3 , NaOH , H_2SO_4 the electrode was further cleaned by Piranha solution before each experimental run. In order to determine the roughness coefficient as depicted in Table 3.1 and the cleanliness of the electrode surface, cyclic voltametry analysis was conducted in 2M H_2SO_4. solution.

Table 3.1. Geometric characteristics of the Au and the Pt electrodes used in the experiment

Electrode	D (mm)	L (mm)	Geometric area	Actual area	Roughness factor
Au 1	0.51	29.23	0.470	1.565	3.327
Au 2	0.46	28.42	0.412	1.394	3.381
Au 3	0.51	28.21	0.454	1.737	3.825
Pt	0.66	27.99	0.584	3.505	6.004

Proper functionalization of the Au electrode is affected by the each step in the self assembly process. Figure 3.4. shows consecutive layers that the assembling procedure comprises of. It is critical to start with a clean gold surface for achieving a successful cystamine mono layer. Since the second and the third steps involve making an amide bond out of an amine and a carboxylic group, a cross linker like EDC is helpful. Once the amine group is combined with the EDC, an unstable ester is formed which is capable of being hydrolyzed back to an amine. As a result, the cross linker alone is not the best way to make a successful amide bond as shown in Figure 3.3. Consequently, sulfo-NHS was also used together with EDC to promote the amide bond. The fourth step involved is the attachment of NAD^+ to the boronic acid ligand. The affinity of the ligand to the cis-diol group depends on the pH of the solution and it is maintained at pH 8-9 as lower pH values make the bond prone to dissociation.

The fuel cell assembled with a functionalized anode and a Pt cathode was used to study the effects of three parameters namely: flow rate , lactate concentration , and the temperature. The values tested for each parameter is represented in the Table 3.2. The standard conditions of 25ml/min substrate flowrate,10mM substrate concentration, and 36 ^{0}C temperature were selected throughout the experimentation. For a particular parameter being tested, the remaining two parameters were kept constant at their standard conditions. The fuel cell was loaded with four external resistors and their values were 100Ω, 1000Ω, 5000Ω and 10000Ω . Under different loading conditions, the load voltage was recorded. The experiment was designed as a split-plot design with three blocks and data were analyzed using statistical software SAS.

Results and discussions

Before running the experiment with the LDH coated electrode an inspection was performed on a sample electrode to ensure that the coating has taken place. Since the changes in the surface takes place at the molecular level, a visible inspection is not at feasible. Consequently, the electrode/s were examined using the scanning electron microscopy. As can be seen in Figure 3.5. the uncoated electrode display evidence of scratch marks of the drawn Au wire. The higher resolution image shows the globular protein matrix that covers the metal surface. The open circuit voltage (OCV) of the cell indicate the potential between the two electrodes when there is no load connected. The effects of the feed flow rate, concentration, and temperature on the OCV is shown in Figure 3.6.(a) , Figure 3.7.(a) and Figure 3.8.(a) respectively. When the feed flow rate changed from 12ml/min to 25ml/min, the OCV did not change significantly and maintained an average value of 266±1mV. When the concentration changed from 1mM to 10mM the OCV did remain unchanged with an average of 256±0.6mV.

Table 3.2. The parameters tested and their respective values.

Flow rate @ 10 m M and 36^{o}C	12ml/min	18ml/min	25/ml/min
Concentration @ 20ml/min @ 36^{o}C	1mM	5mM	10mM
Temperature ^{o}C @ 20 ml/min 10 mM	20	36	40

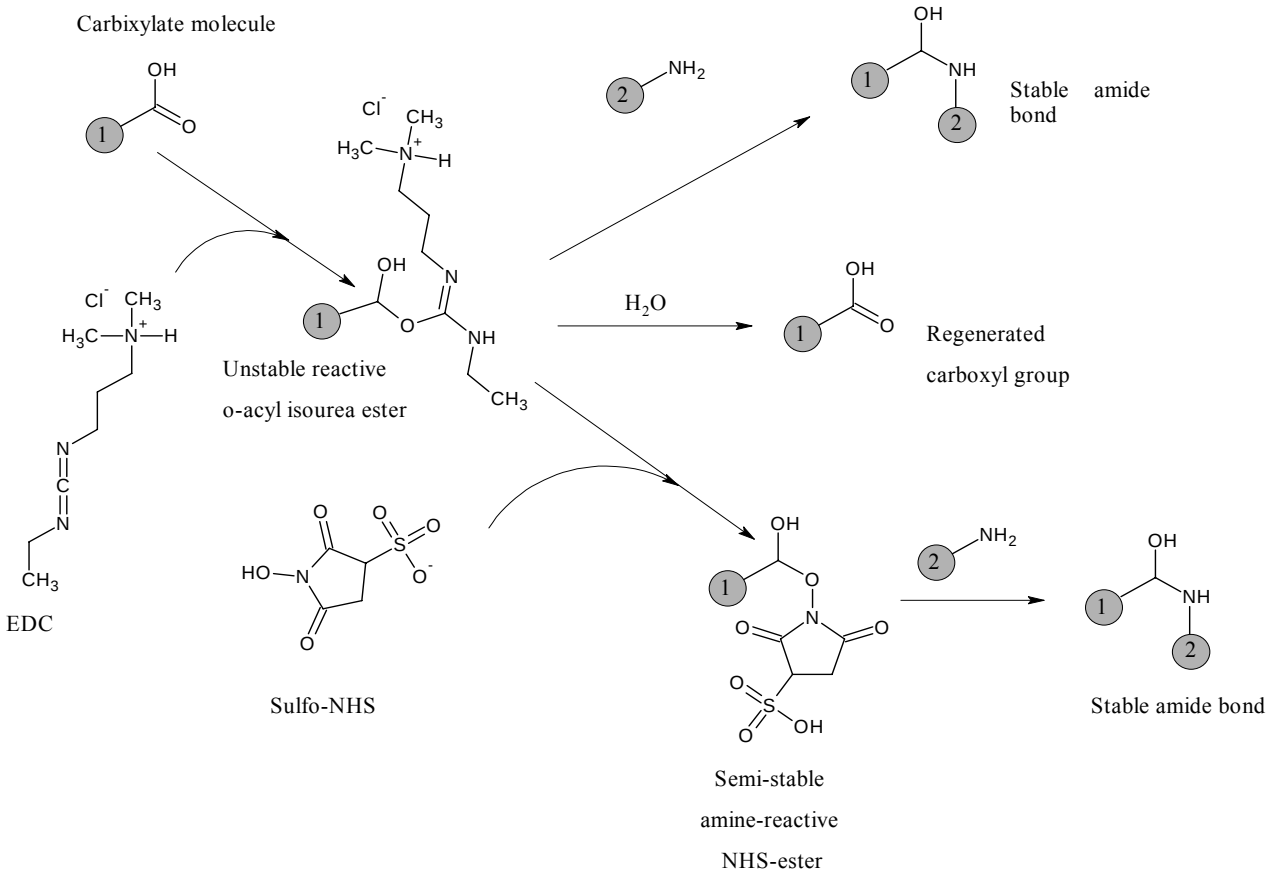

Figure 3.3. EDC and Sulfo-NHS together helps build the amide bond successfully than just EDC or without EDC.[110]

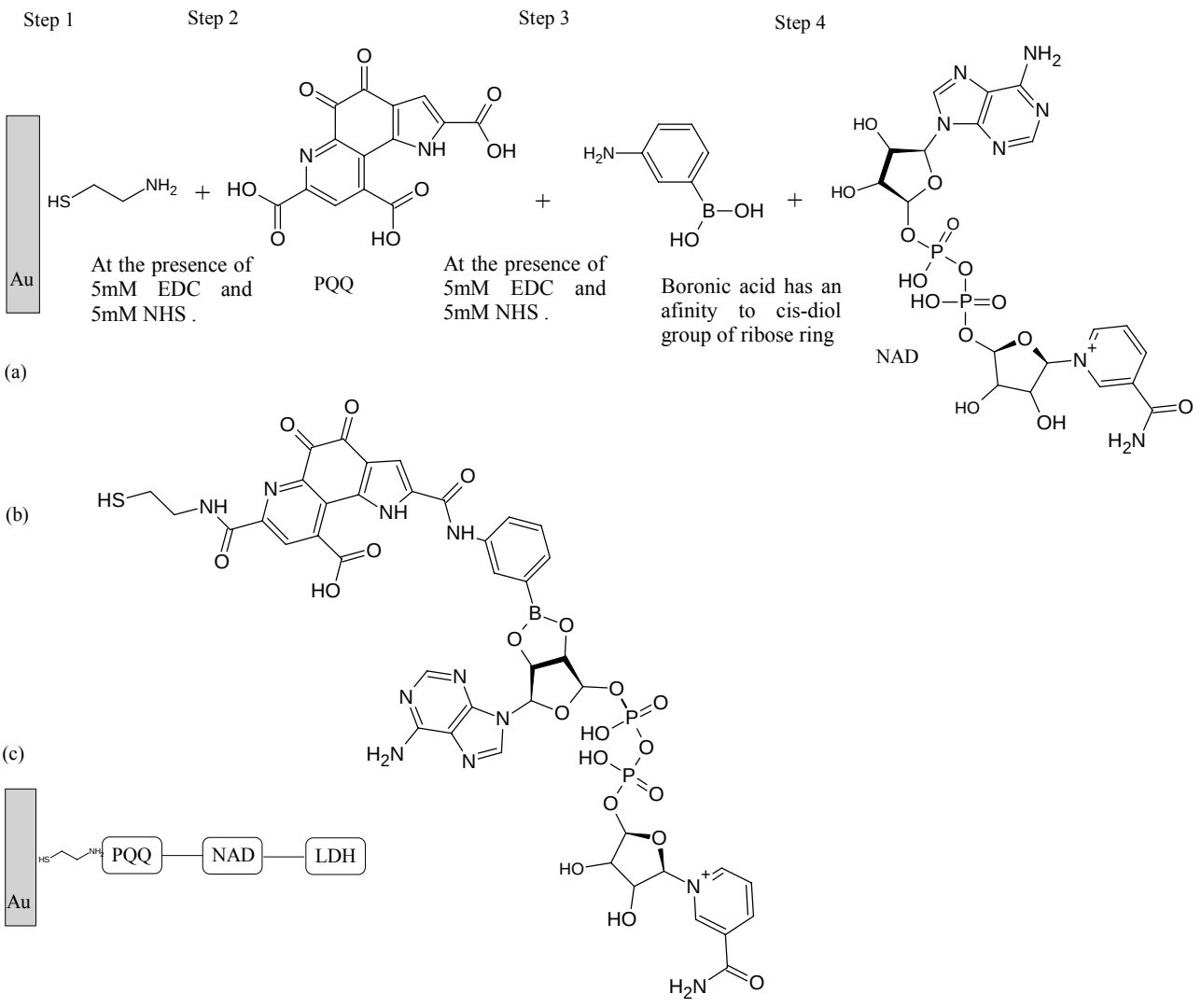

Figure 3.4. The step by step assembly procedure of molecules on to the Au electrode. (a) The involved steps (b) The complete molecular strand when attached (c) The functionalized electrode.

At 20 ^{o}C, the cell reported an OCV of 309±10.1 mV and decreased significantly to 280±4.1 mV when the temperature was increased to 40 ^{o}C. This is some what counter intuitive with respect to the species that the LDH is extracted from. The body temperature of rabbit is in the range of 37^{o}C- 38^{o}C , slightly higher than the human body temperature.

Therefore at 40^{o}C we do not expect a drop in voltage. But studies conducted on rabbit muscle LDH has shown extraordinary behavior at higher temperatures [111].

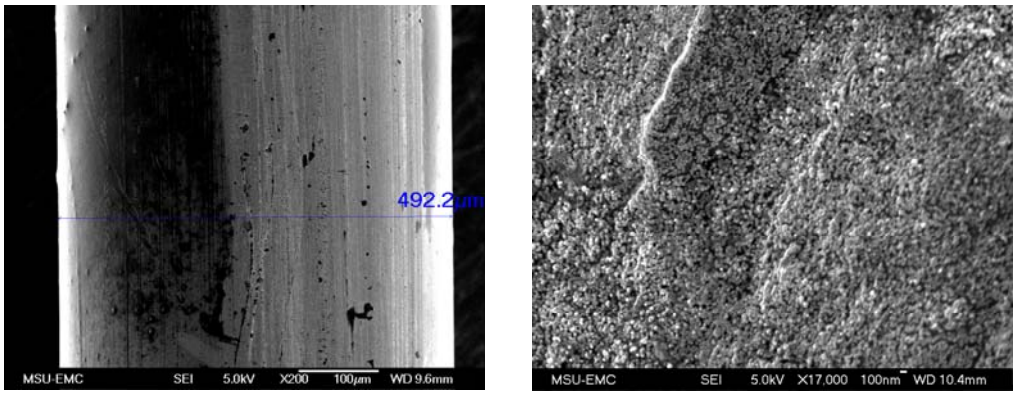

(a) (b)

Figure 3.5. The uncoated and coated gold electrode seen at the scanning electron microscope. (a) Uncoated electrode at a magnification of 200. (b) The gold electrode after coating LDH at a magnification of 17000.

In most enzymes, the K_m (Mechaelis constant) does not increase faster than V_{max} when temperature increases, yet rabbit muscle LDH displays the antitheses. As a result of this enzyme efficiency V_{max}/K_m drops with the increase in temperature. The behavior of the cell under load is significantly different to its open circuit behavior. When there is a current flowing through the cell due to its internal resistance, a substantial amount of energy is dissipated as heat. The current density curves in Figure 3.6.(b) , Figure 3.7.(b) and Figure 3.8. (b) shows distinctive behavior related to feed flow rate , concentration and temperature. When the load is decreased a higher current is drawn by the circuit. At 100Ω in each three figures a maximum current can be observed. When the flow is increased from 12ml/min to 25ml/min there is a significant increase in current density at 100Ω. This explains that the electrode at higher current needs extra support to keep the

mass transfer to the reaction site. By increasing the flow, the mass flow to the electrode is increased and in turn helps improve the current. However, the increasing the lactate concentration from 1mM to 10mM did not show a significant difference in the fuel cell current.

The change in temperature had an important impact on the fuel cell performance especially when the temperature changed from 20^{o}C to 40^{o}C. When the circuit draws a higher current, a higher enzyme turnover rate is required to support the demand. In the Figure 3.8.(b) a clear distinction can be made between the graphs of 20^{o}C and 36^{o}C/ 40^{o}C. At 36^{o}C and 40^{o}C there is no significant difference between the two graphs. Therefore, it could be assumed that the increase in temperature significantly affected the fuel cell when it was loaded.

The power density of the cell showed a similar behavior as the current density. According to Figure 3.6.(c) the power density is high when the external load was 100Ω and also when the flow through the cell was 25ml/min. It is clear from the graphs that the maximum recorded power density of 30.9±1.2 nW/cm^{2}, is steeply declining when the load increases and stays more or less stable thereafter In Figure 3.7.(c) no significant difference can be seen between the graphs of 1mM, 5mM and 10mM which tells that the concentration gradient in that range had no influence on the power density of the fuel cell. The temperature has a similar impact on the power density quite analogous to the current density. In Figure 3.8. (c), it can be seen that at temperatures higher than 20^{o}C, higher power densities were observed. The voltage efficiency of a fuel cell is also an important parameter of the fuel cell performance. Quite contrast to the behavior of the current and the power densities, according to Figure 3.6.(d) , Figure 3.7.(d) and Figure

3.8. (d), the efficiency increased with the increase in load. Under low load conditions when a large current is drawn, the losses involved was higher in comparison to when lower currents were drawn.

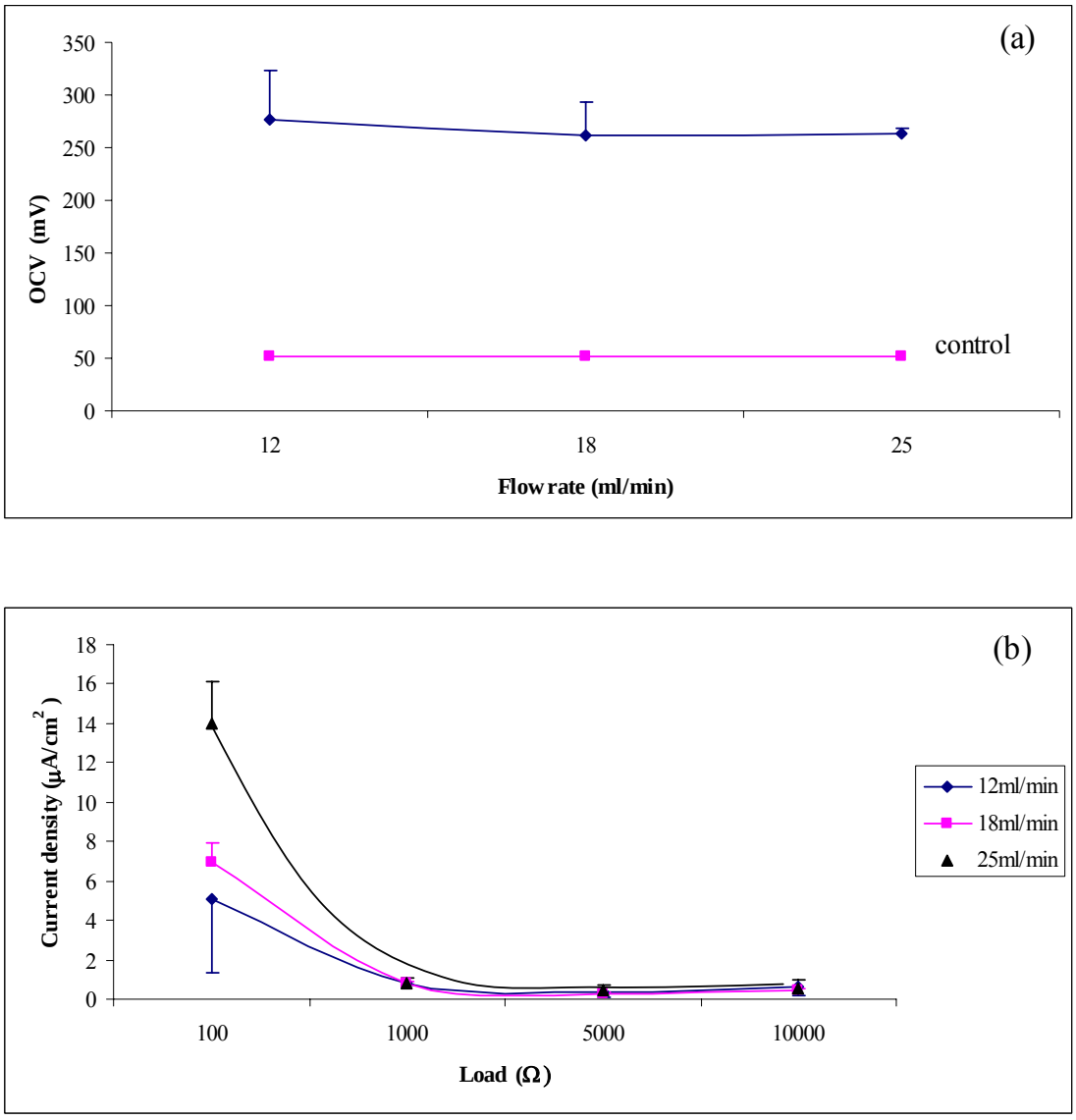

Figure 3.6. The characteristic curves for different feed flow rates 12ml/min, 18ml/min and 25ml/min (a) OCV (b) current density (c) power density (d) efficiency

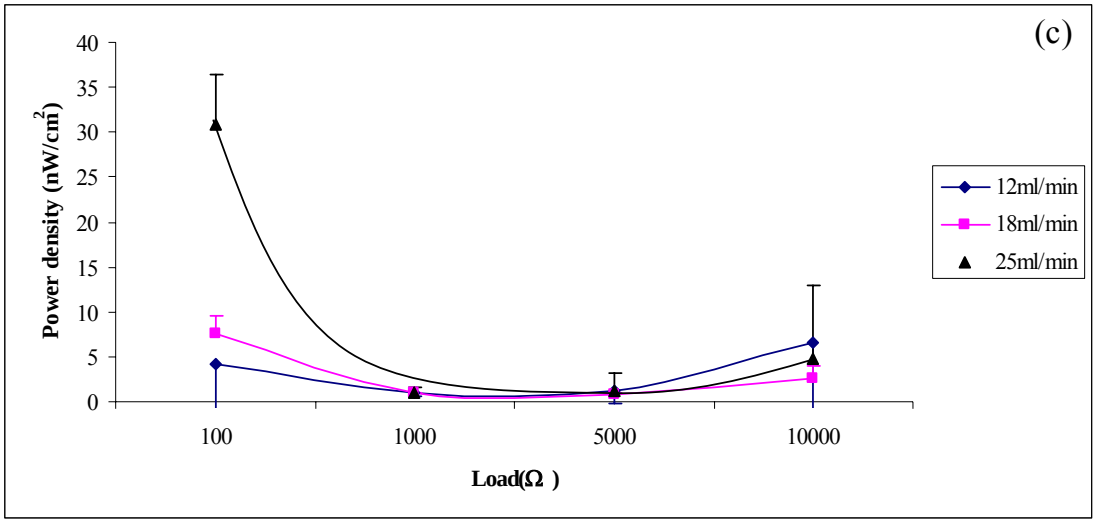

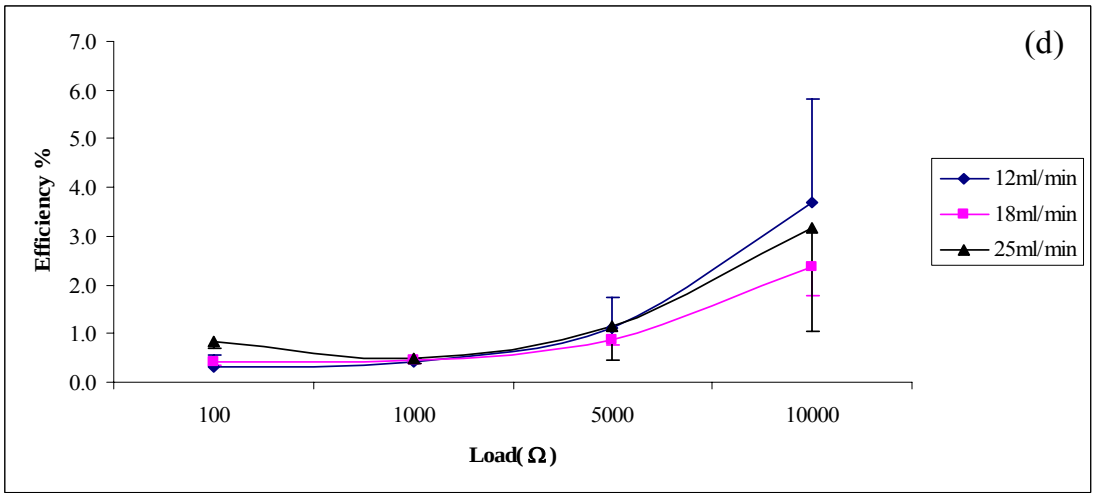

Figure 3.6. (continued)

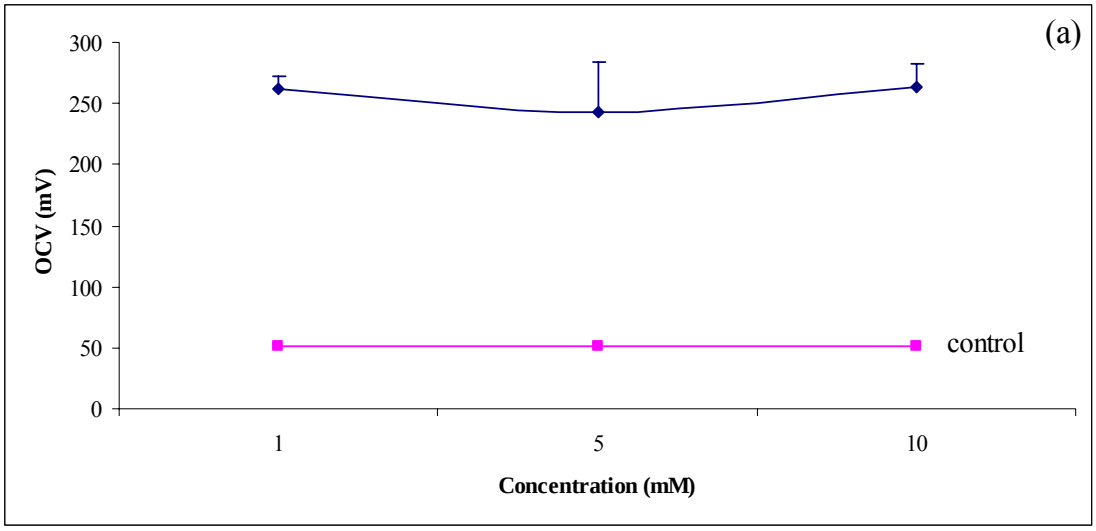

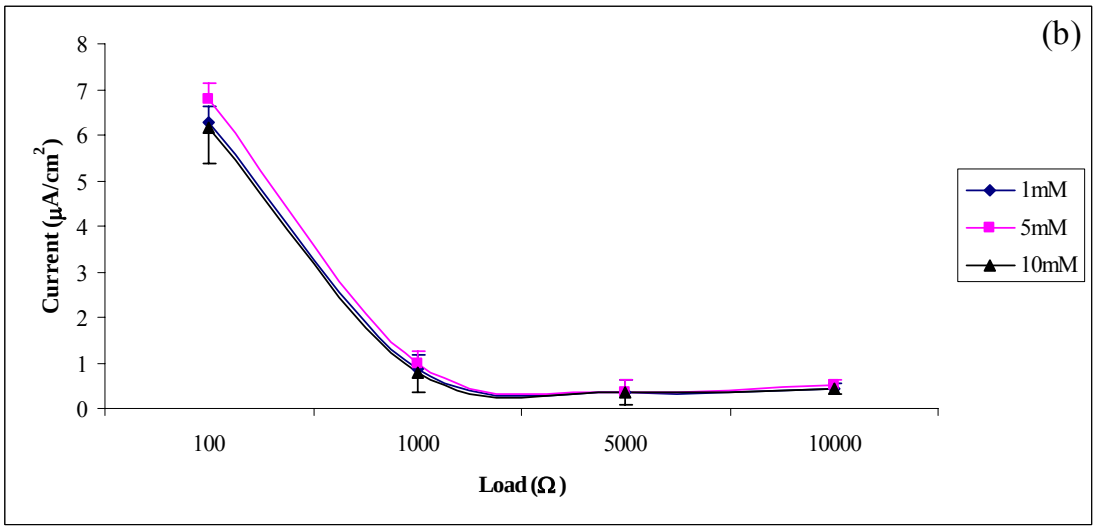

Figure 3.7. Characteristic curve for different concentrations 1mM , 5mM and 10mM. (a) OCV (b) current density (c) power density (d) efficiency

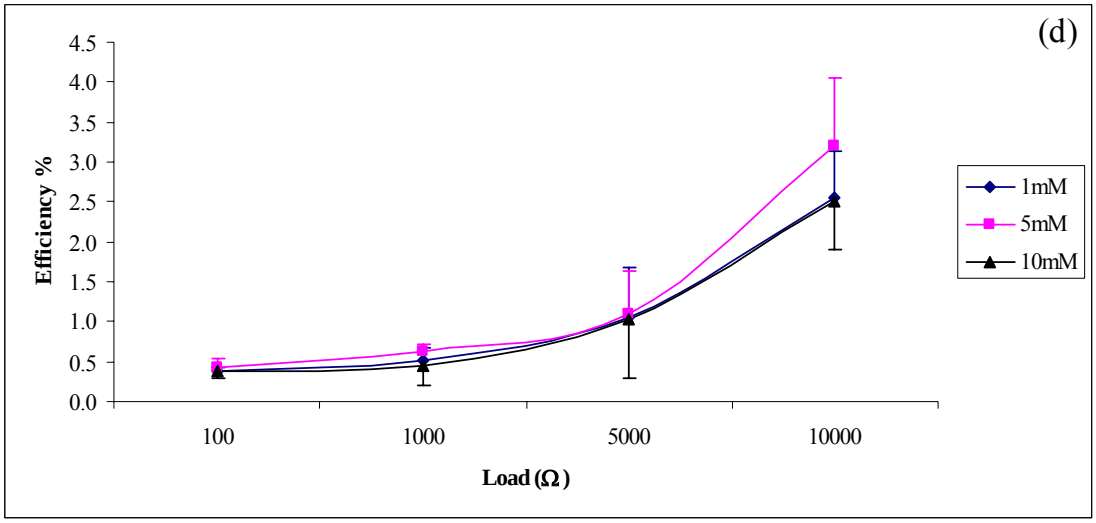

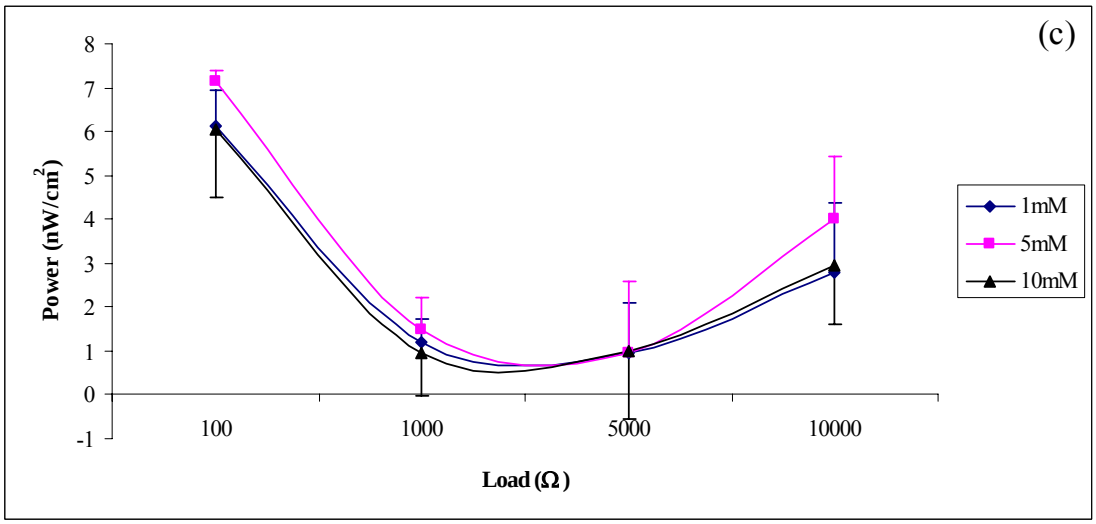

Figure 3.7. (continued)

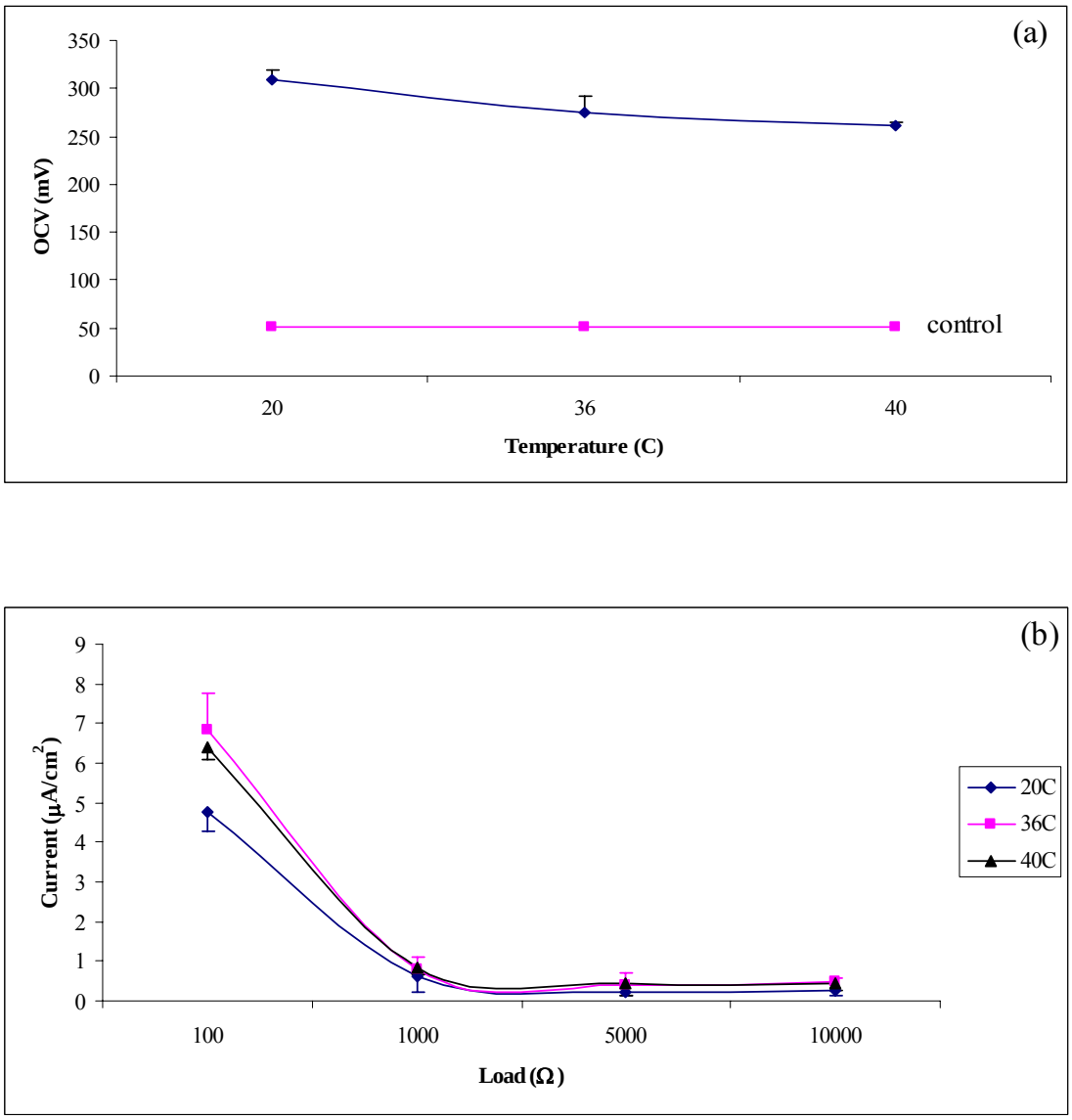

Figure 3.8. Characteristic curves for different temperatures 20°C ,36°C and 40°C. (a) OCV (b) current density (c) power density (d) efficiency

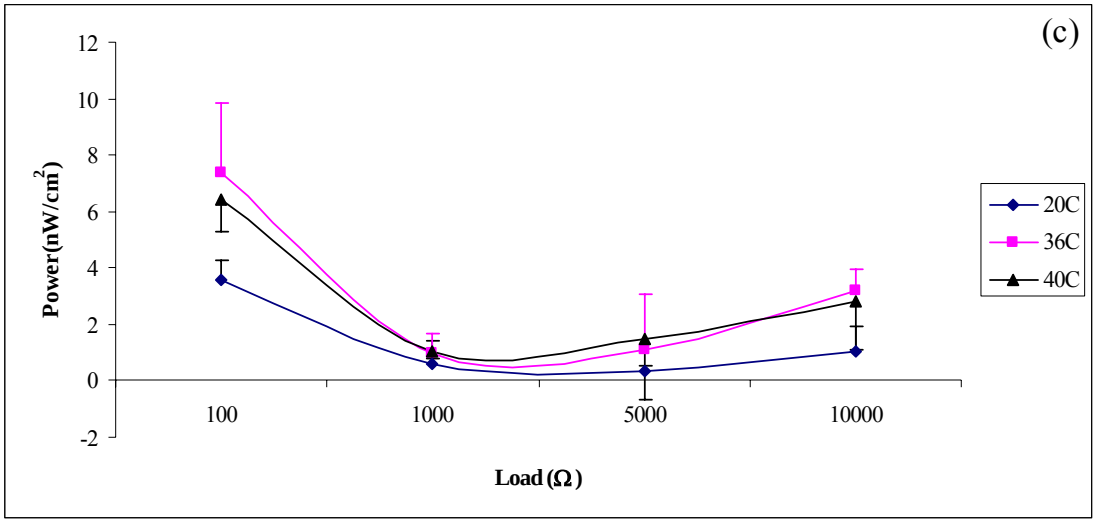

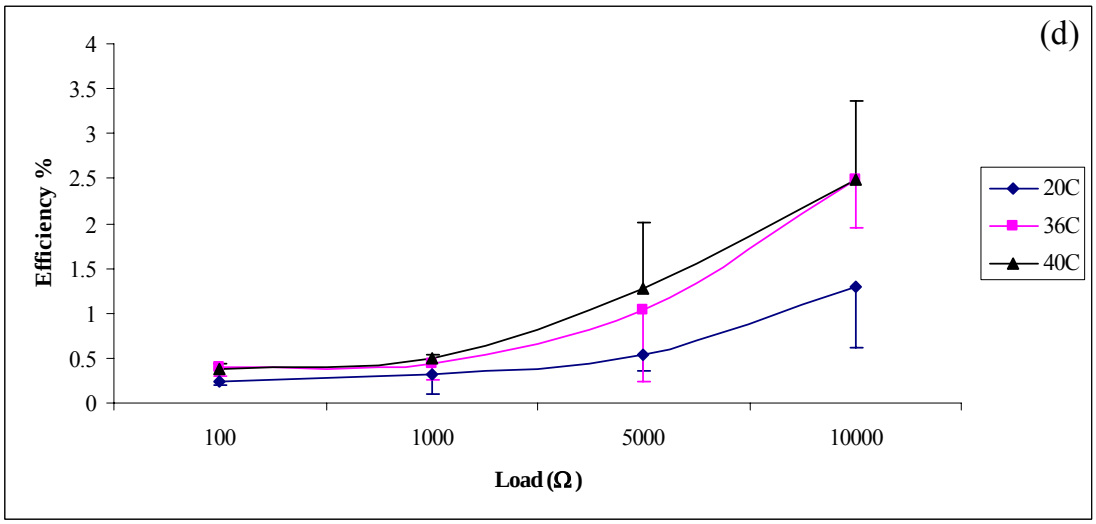

Figure 3.8. (continued)

Conclusions.

The prospect of an enzymatic fuel cell is to be a competitor to all existing micro power devices. In studies so far conducted, there are two main challenges to over come. They are low power densities of the fuel cell and the longevity of the enzyme electrode.

In order to find solutions to these critical issues, it is very important to understand the behavior and the characteristics of different designs. The design we tested resulted in an average OCV of 266±1 mV, power density of 30.9±1.2 nW/cm^2 and an voltage efficiency of 3.6±0.25 %. The results show a high internal resistance of the cell giving way to a steep decline in the voltage. Further improvements in electrical wiring of the enzyme are needed to overcome the intricacies associated with internal resistance.

CHAPTER IV

SUMMARY CONCLUSIONS AND RECOMMENDATIONS

Fuel cells, in general, have become one of the most promising methods to generate electricity. Fuel cells are attractive as compared to the conventional energy generation techniques due to their high energy conversion efficiencies. Usually the efficiency of common types of fuel cells lie in the range of 50%-60%. In addition, factors such as environment friendliness, quietness in operation, and design simplicity adds to its repertoire.

The experiments covered a two-way approach to examine and understand the behavior of biological catalysts in biological fuel cells via a microbial fuel cell and an enzymatic fuel cell.

The Yeast organism used in the biological fuel cell is cheap, stable and easy to replace but when it came the electrical performance, the fungi only displayed a meager aptitude. This is not because they do not under go the redox reactions catalyzing carbohydrates but because of their cellular morphology that hinders charge transport. Consequently, there should be an intermediate molecule to support the electron transfer from the organism to the electrode. According to the observations made from this study, it was apparent that methylene blue caused a significant enhancement in the cell compared to the one without any mediators. According to the results the power density and the efficiency of the fuel cell were 146.71±7.7 mW/m^3, and 26.4% respectively. The

maximum OCV that was obtained was 383.6±1.5 mV. These results portray that the this set-up lacks the required efficiency to be used as a practical fuel cell. The study tells us that more effective electrical communication between the species and the electrode is needed to confront this issue. One particular way to address this issue is to immobilize the mediator on the electrode. Immobilization of the catalyst/microorganism has a better probability of transferring electrons from the species to the electrode. Use of more specific microorganisms such as *ferrireducens* which has iron complexes on its membrane can facilitate charge transfer without the presence of an exogenous mediator. In addition, mutagenesis is a powerful method that could be used in designing new improved species for better transfer of electrons.

Inorganic fuel cells, though successful for macro-scale power generation, is infeasible at the micro scale especially for biological applications. This is because, inorganic fuel cells brings about a multitude of designing, operational and compatibility issues. An enzyme coated electrode has the potential to be miniaturized to the micro levels while circumventing several of the issues present in inorganic fuel cells. Further, the enzymes as catalysts are more specific to the substrate and they are easy to be replaced. For applications like implantable medical devices, such fuel cells have a great potential.

The LDH based enzymatic fuel cell design rendered an efficiency and power density of approximately 3.6±0.25 % and 30.9±1.2nW/cm^2 respectively. The experimented LDH generated an open circuit voltage of 266±1 mV. These values are quite low to compete with the existing sources like dry cells. However, micro devises does not require large amounts of power for operation. For instance, a cardiac pace maker

would consume around 25μW. The enzymatic fuel cell that was developed in this study is a good first step towards this goal. However, the low efficiency of the enzymatic fuel cell has to be circumvented. One way of doing this may be by introducing a longer molecule strand to tether the enzyme on the gold electrode. Cystamine is a chain of two carbons and it holds the protein quite close to the electrode where it will affect dynamics of the enzyme. Tethering the enzyme with a long molecule like β-keratin may help improve the enzyme kinetics and thus may improve the efficiency.

REFERENCES

1. Keneth, L. *Biochemical Fuel Cells*. in *Symposium on Bioelectrochemistry of Microorganisms*. 1966.

2. Oh, S.-E. and B.E. Logan, *Proton exchange membrane and electrode surface areas as factors that affect power generation in microbial fuel cells.* Applied Microbial Biotechnology, 2006. **70**: p. 162-169.

3. Cole, K.S., *Membranes, Ions, and Impulses; A chapter of classical biophysics (Biophysics series)*. 1968, Berkley.: University of California Press. 569.

4. Potter, M.C., *Bacteria as Agents in the Oxidation of Amorphous Carbon.* Proceedings of the Royal Society of London., 1910. **80**(539): p. 239-259.

5. Cohen, B., *The bacterial culture as an electrical half-cell.* Journal of Bacteriology, 1931. **21**: p. 18-19.

6. Wingard, L.B., C.H. Shaw, and J.F. Castner, *Bioelectrochemical Fuel Cells.* Enzyme and Microbial Technology, 1982. **4**(3).

7. Barbir, F., *PEM Fuel Cells: Theory and Practice*. 2005: Elsevier Academic Press. 433.

8. Bennetto, H.P., *Microbial fuel cells.* Life chemistry report., 1984. **2**(4): p. 363-453.

9. Bennetto, H.P., *Electricity generation by microorganisms.* Biotechnology Education, 1990. **1**: p. 163-168.

10. Aston, W.J. and A.P.F. Turner, *Biosensors and biofuel cells.* Biotechnology and Genetic Engineering Reviews 1, 1984(1): p. 89.

11. White, A., P. Handler, and E.L. Smith, *Principle Biochemistry*, ed. 5. 1973: McGraw Hill.

12. Cooney, M.J., R. E, and M.I. W, *Physiologic studies with sulfate-reducing bacterium desulfovibrio desulfuricans.* Enzyme and Microbial Technology, 1996. **18**(5): p. 358-365.

13. Scholz, F. and U. Schroder, *Bacterial Batteries.* Nature Biotechnology, 2003. **21**(10): p. 1151-1152.

14. Tender, L.M., *Harnessing microbially generated power on the seafloor.* Nature Biotechnology, 2002. **20**(8): p. 821-825.

15. Roller, S.D., *Electron transfer coupling in microbial fuel-cells. 1.Comparison of redox-mediator reduction rates and respiratory rates of bacteria.* Journal of Chemical Technology and Biotechnology, 1984. **34B**: p. 3-12.

16. Park, D.H. and J.G. Zeikus, *Improved fuelcell and electrode designs for producing electricity from microbial degradation.* Bioenergy and Biotechnology, 2003. **81**(3): p. 384-355.

17. Willner, I., E. Katz, P. F, and A.F. Buckmann, *Biofuel cell based on glucose oxidase and microperoxidase-11 monolayer-functionalized electrodes.* Journal of Chemical Society-Perkin Transaction 2, 1998(2): p. 1817-1822.

18. Delaney, G.M., H.P. Bennetto, J.R. Mason, S.D. Roller, J.L. Stirling, and C.F. Thurston, *Electron-transfer coupling in microbial fuel-cells. 2. Performance of fuel-cells containing selected microorganism mediator substrate combination.* Journal of Chemical Technology and Biotechnology, 1984. **34**(1): p. 13-27.

19. Gil, G.C., I. Chang, B.H. Kim, M. Kim, J.-K. Jang, H.S. Park, and H.J. Kim, *Operational parameters affecting the performance of a mediator-less microbial fuel cell.* Biosensors and bioelectronics, 2003. **18**(4): p. 327-334.

20. Chaudhuri, S.K. and D.R. Loveley, *Electricity generation by direct oxidation of glucose in mediatorless microbial fuel cells.* Nature Bio Technology, 2003(21): p. 1229-1232.

21. Rabaey, K., G. Lissens, S.D. Siciliano, and W. Verstraete, *A microbial fuelcell capable of converting glucose to electricity at high rate and efficiency.* Biotechnology Letters, 2003. **25**: p. 1531-1535.

22. Larminie, J. and A. Dicks, *Fuelcell system explained.* 2000: John Wiley & Sons. 406.

23. Schroder, U., J. Niessen, and F. Scholz, *A generation of microbial fuel cells with current outputs boosted by more than one order of magnitude.* Angewandte Cheme International Edition, 2003. **42**(25): p. 2880-2883.

24. Rhoads, A., H. Beynal, and Z. Lewandowski, *Microbial Fuel Cell using Anaerobic Respiration as an Anodic Reaction and Biomineralized Manganese as a Cathodic Reactant.* Environmental Science and Technology, 2005. **39**: p. 4666-4671.

25. Liu, H., S. Cheng, and B.E. Logan, *Power Generation in Fed-Batch Microbial Fuel Cells as a function of Ionic Strength, Temperature, and Reactor Configurations.* Environmental Science and Technology, 2005. **39**: p. 5488-5493.

26. Jang, J.K., *Construction and operation of a novel mediator and membraneless microbial fuel cell.* Process Biochemistry, 2004. **38**(8): p. 1007-1012.

27. Pizzariello A, Stredansky M, and M. S., *A glucose/hydrogen peroxide biofuel cell that uses oxidase and peroxidase as catalysts by composite bulk-modified bioelectrodes based on a solid binding matrix.* Bioelectrochemistry, 2002. **56**: p. 99– 105.

28. Allen, R.M. and H.P. Bennetto, *Microbial Fuel-Cells electricity production from carbohydrates.* Applied Biochemical and Biotechnology, 1993. **40**: p. 27-40.

29. Bartlett, P.N., Caruana, D.J., *Electrochemical immobilization of enzymes. Part V. Microelectrodes for the detection of glucose based on glucose oxidase immobilized in a poly(phenol) film.* Analyst, 1992. **117**: p. 1287–1292.

30. Bartlett, P.N., Whitaker, R.G., *Strategies for the development of amperometric enzyme electrodes.* Biosensors, 1988(3): p. 359–379.

31. Maria Jesús Lobo, Arturo J. Miranda, and P. Tuñón, *Amperometric biosensors based on NAD(P)-dependent dehydrogenase enzymes.* Electroanalysis, 2005. **9**(3): p. 191-202.

32. Shelley D Minteer, B.Y. Liaw, and M.J. Cooney, *Enzyme-based biofuel cells.* Current Opinion in Biotechnology, 2007(18): p. 1-7.

33. Yashiro, A.T., S.M. Lee, and K.D. O, *Bioelectrochemistry Enzyme utilizing biofuel cell studies.* Biochemica et Biophysica acta, 1964. **88**: p. 375.

34. Dijik, C.V., C. Laane, and C. Veeger, *Biochemical fuel cells and amperometric biosensors.* Rcl. Trav. Chim Pays-Bas, 1985(104): p. 245.

35. Bartlett, P.N., P. Tebbutt, and R.C. Whitaker, *Kinetic aspects of the use of modified electrodes and mediators in bioelectrochemistry.* Prog. Reaction Kinetics, 1991(16): p. 55.

36. Willner, I. and E. Katz, *Integration of Layered Redox Proteins and Conductive Supports for Bioelectronic Applications.* Angewandte Cheme International Edition, 2000. **39**: p. 1180-1218.

37. Armstrong, F.A., H.A.O. Hill, and N.J.Q. Walton, *Reactions of electron-transfer proteins at electrodes.* Quarterly reviews of biophysics, 1985. **18**(3): p. 261-322.

38. Pardo-Yissa, V., E. Katz, I. Willner, A.B. Kotlyar, C. Sanders, and H. Lill, *Biomaterial engineered electrodes for bioelectronics.* Faraday Discussions, 2000. **116**: p. 119-134.

39. Willner, I., V. Heleg-Shabtai, R. Blonder, E. Katz, and G. Tao, *Electrical Wiring of Glucose oxidase by Reconstitution of FAD-Modified monolayers Assembled onto Au- Electrodes.* Journal of American Chemical Society, 1996. **118**: p. 10321-10322.

40. Allen, H. and O. HIll, *Bio-electrochemistry.* Pure & App. Chem., 1987. **59**(6): p. 743-748.

41. Albery, W.J., M.J. Eddowes, H.A.O. Hill, and A.R. Hillmann, *Mechanism of the reduction and oxidation reaction of cytochrome c at a modified gold electrode.* Journal of American Chemical Society, 1981. **103**: p. 3904—3910.

42. Ghindilis, A.L., P. Antanasov, and E. Wilkins, *Enzyme-catalyzed direct electron transfer: Fundamentals and analytical applications.* Electroanalysis, 1997. **9**(9): p. 661-667.

43. Allen, M.J., J.R. Norris, and D.W. Ribbons, *Methods in microbiology. Academic Press*. 1972. 247-283.

44. Solomon, E.I., U.M. Sundaram, and T.E. Machonkin, *Multicopper Oxidases and Oxygenases.* Chemical Review, 1996(96): p. 2563.

45. Gupta, G., V. Ragendran, and P. Atanassov, *Bioelectrocatalysis of oxygen reduction reaction by laccase on gold electrodes.* Electroanalysis, 2004(16): p. 1182.

46. Palmore, G.T.R., G.M. Whitesides, S.H. Bergens, and H. Bertschy, *A methanol/dioxygen biofuel cell that uses NAD+-dependent dehydrogenases as catalysts: application of an electro-enzymic method to regenerate nicotinamide adenine dinucleotide at low overpotentials.* Electro analytical chemistry, 1998. **443**(1): p. 155-161.

47. Palmore, G.T.R. and H.H. Kim, *Electro-enzymatiic reduction of dioxygen to water in the cathode compartment of a biofuel cell.* Journal of Electroanalytical chemistry, 1999. **464**: p. 110-117.

48. Brenda. *The database for Enzymes and their nomenclature*. [cited; Available from: http://www.brenda-enzymes.info.

49. Bullen, R.A., T.C. Arnot, J.B. Lakeman, and F.C. Walsh, *Biofuelcells and their development.* Biosensors and bioelectronics, 2006. **21**: p. 2015-2045.

50. Katakis, I., *Catalytic electrooxidation of NADH for dehydrogenase amperometric biosensors.* Microchim Acta, 1997. **126**: p. 11-32.

51. Persson, B., L. Gorton, G. Johansson, and A. Torstensson, *Biofuel anode based on D-glucose dehydrogenase, nicotinamide adenine dinucleotide and a modified electrode.* Enzyme and Microbial Technology, 1985. **7**(11): p. 549-552.

52. Topcagic, S., B.L. Treu, and S.D. Minteer, *Alcohol -based biofuel cells.* Industrial and Engineering Chemistry, 2006(112): p. 215-231.

53. Akers, N.L., C.M. Moore, and S.D. Minteer, *Development of alcohol/O2 biofuel cells using salt-extracted tetrabutylammonium bromide/Nafion membranes to immobilize dehydrogenase enzymes.* Electrochim acta, 2005. **50**(12): p. 2521-2525.

54. Zhang, X.-C., A. Ranta, and A. Halme, *Direct Methonol Biocatalytic fuel cell Considerations of restraints on electron transfer.* Biosensors and bioelectronics, 2006. **21**: p. 2052-2057.

55. Liu, Y., M. Wang, F. Zhao, B. Liu, and S. Dong, *A low cost biofuel cell with Ph-dependent power output based on porous carbon as matrix.* Chemical Europian Journal, 2005. **11**: p. 4970-4974.

56. Mano N, Mao F, and H. A., *A miniature biofuel cell operating in a physiological buffer.* J Am Chem Soc, 2002. **124**: p. 12962.

57. Tsujimura, S., B. Tatsumi, J. Ogawa, S. Shimizu, K. Kano, and T. Ikeda, *Bioelectrocatalytic reduction of dioxygen to water at neutral pH using bilirubin oxidase as an enzyme and 2,2'-azinobis (3-ethylbenzothiazolin-6-sulfonate) as an electron transfer mediator.* Journal of Electroanalytical chemistry, 2001. **496**(1-2): p. 69.

58. Katz, E., I. Willner, A. Riklin, V. Heleg-Shabtai, and A.F. Buckmann, *Glucose oxidase electrodes via reconstitution of the apo-enzyme: tailoring of novel glucose biosensors.* Analytica Chimica Acta, 1999. **385**: p. 45-58.

59. Karyakin, A.A., E.E. Karyakina, and H.L. Schimdt, *Electropolymerized Azines: A New Group of Electroactive Polymers.* Electroanalysis, 1999. **3**(11): p. 149.

60. Willner, I., A. G, and E. Katz, *A biofuel cell based on pyrroloquinoline quinone and microperoxidase-11 monolayer-functionalized electrodes.* Bioelectrochemical Bioenerg., 1998. **44**(2): p. 209-214.

61. Tarasevich MR, Bogdanovskaya VA, Zagudaeva NM, and K. AV., *Composite materials for direct bioelectrocatalysis of the hydrogen and oxygen reactions in biofuel cells.* Russ J Electrochem, 2002. **38**: p. 335.

62. Moore CM, Akers NL, Hill AD, Johnson ZC, and M. SD., *Improving the environment for immobilized dehydrogenase enzymes by modifying nafion with tetraalkylammonium bromides.* Biomacromolecules, 2002. **5**: p. 1241– 1247.

63. Katz, E., I. Willner, and A.B. Kotlyar, *A non-compartmentalized glucose O_2 biofuel cell by bioengineered electrode surfaces.* Electroanalytical Chemistry, 1999(479): p. 64-68.

64. Willner, I. and A. Riklin, *Electrical Communication between Electrodes and NAD(P)+-Dependent Enzymes Using Pyrroloquinolinequinone-Enzyme Electrodes in a Self-Assembled Monolayer Configuration: Design of a New Class of Amperometric Biosensors.* Analytical Chemistry, 1994. **66**(9): p. 1535-1539.

65. Widrig, C. and M. Majda, *Mediated, thin-layer cell, coulometric determination of monomolecular films of trichlorosilane viologen derivatives at gold and non conducting surfaces.* Analytical Chemistry, 1987. **59**(5): p. 754-760.

66. Proctor, A., J.F. Castner, L.B. Wingard, and D.M. Hercules, *Electron spectroscopic (ESCA) studies of platinum surfaces used for enzyme electrodes.* Analytical Chemistry, 1985. **57**(8): p. 1644-1649.

67. Angerstein-Koslowska, H., B.E. Conway, and W.B.A. Sharp, *The real condition of electrochemically oxidized platinum surfaces: Part I. Resolution of component processes.* Journal of Electroanalytical chemistry, 1973. **43**(1): p. 9-36.

68. Burke, L.D. and M.B.C. Roche, *Hydrous oxide formation on platinum—A useful route to controlled platinization.* Journal of Electroanalytical chemistry, 1984. **164**(2): p. 315-334.

69. Facci, J. and R.W. Murray, *Silanization and non-aqueous electrochemistry of two oxide states on platinum electrodes.* Journal of Electroanalytical Chemistry, 1980. **112**(2): p. 221-229.

70. Lenhard, J.R. and R.W. Murray, *Chemically modified electrodes Part VII. Covalent bonding of a reversible electrode reactant to Pt electrodes using an*

organosilane reagent. Journal of Electroanalytical Chemistry, 1977. **78**(1): p. 195-201.

71. Bain, C.D., E.B. Troughton, Y.T. Tao, J. Eval, G.M. Whiteside, and R.G. Nuzzo, *Formation of monolayer films by the spontaneous assembly of organic thiols from solution onto gold.* Journal of American Chemical Society, 1989. **111**(1): p. 321-335.

72. Nuzzo, R.G., F.A. Fusco, and D.L. Allara, *Spontaneously organized molecular assemblies. 3. Preparation and properties of solution adsorbed monolayers of organic disulfides on gold surfaces.* Journal of American Chemical Society, 1987. **109**(8): p. 2358-2368.

73. Throughton, E.B., C.D. Bain, G.M. Whiteside, R.G. Nuzzo, D.L. Allara, and M.D. Porter, *Monolayer films prepared by the spontaneous self-assembly of symmetrical and unsymmetrical dialkyl sulfides from solution onto gold substrates: structure, properties, and reactivity of constituent functional groups.* Langmuir, 1988. **4**(2): p. 365-385.

74. Katz, E., N. Itzhak, and I. Willner, *Effects of monolayer packing on the electrochemical activity of chemisorbed thioderivatized N,N'-dialkyl-4,4'-bipyridinium.* Journal of Electroanalytical Chemistry, 1992. **336**(1-2): p. 357-562.

75. Beulen, M.W.J., B.H. Huisman, P.A.v.d. Heijden, C.F.J.M.v. Veggel, M.G. Simons, E.M.E.F. Biemond, P.J.d. Lange, and D.N. Reinhoudt, *Evidence for Nondestructive Adsorption of Di-alkyl Sulfides on Gold.* Langmuir, 1996. **12**(26): p. 6170-6172.

76. Delamarche, E., B. Michel, H.A. Biebuyck, and C. Gerber, *Golden interfaces: The Surface of Self-Assembled Monolayers.* Advance Materials, 1996. **8**(9): p. 719-729.

77. Nuzzo, R.G., B.R. Zegarski, and L.H. Dubois, *Fundamental studies of the chemisorption of organosulfur compounds on gold(111). Implications for molecular self-assembly on gold surfaces.* Journal of American Chemical Society, 1987. **109**: p. 733-740.

78. Hickman, J.J.Z., Chaofeng; Ofer, David; Harvey, Pierre D.; Wrighton, Mark S.; Laibinis, Paul E.; Bain, Colin D.; Whitesides, George M., *Combining*

spontaneous molecular assembly with microfabrication to pattern surfaces: selective binding of isonitriles to platinum micro wires and characterization by electrochemistry and surface spectroscopy. Journal of the American Chemical Society, 1989. **111**(18): p. 7271-7272.

79. Walczak, M.M.C., Chinkap; Stole, Scott M.; Widrig, Cindra A.; Porter, Marc D., *Structure and interfacial properties of spontaneously adsorbed n-alkanethiolate monolayers on evaporated silver surfaces.* Journal of the American Chemical Society, 1991. **113**(7): p. 2370-2378.

80. Katz, E., D.D. Schlereth, and H.L. Schmidt, *Electrochemical study of pyrroloquinoline quinone covalently immobilized as a monolayer onto a cystamine-modified gold electrode.* Journal of Electroanalytical chemistry, 1994. **367**: p. 59-70.

81. Katz, E., Maya Zayats, and I. Willner, *Electrical Contacting of Flavoenzymes and NAD(P)+-Dependent Enzymes by Reconstitution and Affinity Interactions on Phenylboronic Acid Monolayers Associated with Au-Electrodes.* J Am Chem Soc, 2002. **124**: p. 14724-14735.

82. Katz, E. and I. Willner, *A Biofuel Cell with Electrochemically Switch able and Tunable Power Output.* J. Am. Chem. Soc., 2003. **125**: p. 6803-6813.

83. Katz, E., V. Heleg-Shabtai, A. Bardea, I. Willner, H.K. Rau, and W. Haehnel, *Fully integrated biocatalytic electrodes based on bioaffinity interactions1.* Biosensors & Bioelectronics, 1998. **13**: p. 741–756.

84. Katz, E., T. Lotzbeyer, D.D. Schlereth, W. Schuhmann, and H.L. Schimdt, *Electrocatalytic oxidation of reduced nicotinamide coenzymes at gold and platinum electrode surfaces modified with a monolayer of pyrroloquinoline quinone. Effect of Ca2+ cataions.* Journal of Electroanalytical Chemistry, 1994. **373**: p. 189.

85. Katz, E., A.N. Shipway, and I. Willner, *Biochemical fuel cells*. Handbook of Fuel Cells: Fundamentals, Technology, Applications, ed. Wolf Vielstich (Editor), Arnold Lamm (Editor), and H.G. (Editor). 2003.

86. Kharitonov, A.B., L. Alfonta, E. Katz, and I. Willner, *Probing of bioaffinity interactions at interfaces using impedance spectroscopy and chronopotentiometry.* Journal of Electroanalytical chemistry, 2000. **487,** (2): p. 133-141.

87. Duke, C.B. and L.B. Shein, *Organic Solids: is energy based theory enough?* Phys. Today, 1980. **33**: p. 42-48.

88. Bloor, D. and B. Movaghar, *Conducting polymers.* IEEE Proceedings, 1983. **130**: p. 225-232.

89. Situmorang, M., J.J. Gooding, D.B. Hibert, and D. Barnet, *Electrodeposited polytyramine as an immobilization matrix for enzyme biosensors.* Biosensors & Bioelectronics, 1998. **13**(9): p. 953-962.

90. Trojanowicz, M.K., Tadeusz; Krawczynski vel Krawczyk, Tadeusz., *Electrochemical biosensors based on enzymes immobilized in electropolymerized films.* Mikrochimica Acta, 1995. **121**(1-4): p. 167-181.

91. Wring, S.A.H., John P., *Chemically modified, carbon-based electrodes and their application as electrochemical sensors for the analysis of biologically important compounds. A review.* Analyst (Cambridge, United Kingdom), 1992. **117**(8): p. 1215-1229.

92. Forzani, E.S.O., Marcelo; Perez, Manuel A.; Teijelo, Manuel Lopez; Calvo, Ernesto J., *The Structure of Layer-by-Layer Self-Assembled Glucose Oxidase and Os(Bpy)2ClPyCH2NH-Poly(allylamine) Multilayers: Ellipsometric and Quartz Crystal Microbalance Studies.* Langmuir, 2002. **18**(10): p. 4020-4029.

93. Rajagopalan, R.H., A., *Electrical "wiring" of glucose oxidase in electron conducting hydrogels.* Molecular Electronics, 1997: p. 241-254.

94. Merchant, S.A., D.T. Glatzhofer, and D.W. Schmidtke, *Effects of Electrolyte and pH on the Behavior of Cross-Linked Films of Ferrocene-Modified Poly(ethylenimine).* Langmuir, 2007. **23**(22): p. 11295 -11302.

95. Zhiqiang, G., B. Gary, K. Hyug-Han, B.S. Calabrese, Z. Yongchao, and H. Adam, *Electrodeposition of redox polymers and co-electrodeposition of enzymes by coordinative crosslinking.* Angewandte Chemie (International ed. in English), 2002. **41**(5): p. 810-813.

96. Chaubey, A.G., M.; Singhal, R.; Singh, V. S.; Malhotra, B. D., *Immobilization of lactate dehydrogenase on electrochemically prepared polypyrrole-polyvinylsulphonate composite films for application to lactate biosensors.* Electrochimica Acta, 2000. **46**(5): p. 723-729.

97. Chaubey, A.P., K. K.; Singh, V. S.; Malhotra, B. D., *Co-immobilization of lactate oxidase and lactate dehydrogenase on conducting poly aniline films.* Analytica Chimica Acta, 2000. **407**(1-2): p. 97-103.

98. James Lim, P.M., Francois Bonet, and Bruce Dunn, *Nanostructured Sol-Gel Electrodes for Biofuel Cells.* J. Electrochem. Soc., 2007. **154,**(2): p. 140-145.

99. Shukla, A.K., P. Suresh, S. Berchmans, and A. Rajendran, *Biological fuel cells and their applications.* Current Science, 2004. **81**(4).

100. Bond, D.R. and D.R. Loveley, *Electricity production by Geobacter Sulfurreducens attached to electrodes.* Applied Environmental Microbiology, 2003. **69**: p. 1548-1555.

101. Kim, B.H., H.S. Park, H.J. Kim, G.T. Kim, I.S. Chang, J. Lee, and N.T. Phung, *Enrichment of microbial community generating electricity using a fuel-cell-type electrochemical cell.* 2004(63): p. 672-681.

102. Kim, B.H., H.J. Kim, M.S. Hyun, and D.H. Park, *Direct electrode reaction of Fe(III) -reducing bacterium, Shewanella putrefaciens.* Journal of Microbial Technology, 1999. **19**: p. 127-131.

103. Feldmann, H., *Yeast Molecular Biology - (A Short Compendium on Basic Features And Novel Aspects.)*. 2005, Adolf-Butenandt-Institute University of Munich.

104. Nelson, D.L. and M.M. Cox, *Principles of Biochemistry*. 4 ed. Lehninger. 2005.

105. Bard, A.J. and L.R. Faulkner, *Electrochemical Methods: Fundamentals and Applications*. 2 ed. 2001.

106. Barton, S.C., J. Gallaway, and P. Atanassov, *Enzymatic Biofuel Cells for Implantable and Micro scale Devices.* Chemical Review, 2004. **104**: p. 4867-4886.

107. Wouassi, D., J. Mercier, S. Ahmaidi, J. F. Brun, B. Mercier, A. Orsetti, and C. Préfaut, *Metabolic and hormonal responses during repeated bouts of brief and intense exercise: effects of pre-exercise glucose ingestion.* European Journal of Applied Physiology and Occupational Physiology, 1997. **76**(3): p. 197-202.

108. Yuhashi, N., M. Tomiyama, J. Okuda, S. Igarashi, K. Ikebukuro, and K. Sode, *Development of a novel glucose enzyme fuel cell system employing protein engineered PQQ glucose dehydrogenase.* Biosensors and bioelectronics, 2005. **20**: p. 2145-2150.

109. Amos Bardea, Eugenii Katz, Andreas F. Buckmann, and I. Willner, *NAD+-Dependent Enzyme Electrodes: Electrical Contact of Cofactor-Dependent Enzymes and Electrodes.* J. Am. Chem. Soc., 1997. **119**: p. 9114-9119.

110. Proteins. *Protein and its chemistries*. [cited; Available from: http://www.piercenet.com/.

111. Scopes, R.K., *The effect of temperature on enzymes used in diagnostics.* Clinica Chimica Acta, 1995. **237**(1-2): p. 17.

APPENDIX A

STATISTICAL DATA ANALYSIS FOR THE YIEST FUEL CELL

The SAS output for the multiple comparisons for treatment combinations with voltage as the output.

Alpha	0.05
Error Degrees of Freedom	282
Error Mean Square	2.699E-6
Critical Value of t	1.96841
Least Significant Difference	0.0007

t Grouping	Mean	N	TRT
A	0.2186069	48	[1KΩ,EX2]
B	0.0744628	48	[1KΩ,EX6]
C	0.0414019	48	[1KΩ,EX1]
D	0.0377912	48	[1KΩ,EX4]
E	0.0350833	48	[1KΩ,EX3]
F	0.0244142	48	[1KΩ,EX5]

Alpha	0.05
Error Degrees of Freedom	138
Error Mean Square	2.264E-6
Critical Value of t	1.97730
Least Significant Difference	0.0009

t Grouping	Mean	N	TRT
A	0.3177867	24	[10KΩ,EX2]
B	0.2039550	24	[10KΩ,EX1]
C	0.1795950	24	[10KΩ,EX6]
D	0.1537000	24	[10KΩ,EX3]
E	0.1463833	24	[10KΩ,EX4]
F	0.1293467	24	[10KΩ,EX5]

Alpha	0.05
Error Degrees of Freedom	174
Error Mean Square	0.00016
Critical Value of t	1.97369
Least Significant Difference	0.0064

t Grouping	Mean	N	TRT
A	0.340284	30	[100KΩ,EX1]
B	0.323571	30	[100KΩ,EX2]
C	0.287753	30	[100KΩ,EX3]
D	0.265485	30	[100KΩ,EX5]
E	0.211383	30	[100KΩ,EX4]
E			
E	0.206178	30	[100KΩ,EX6]

The SAS output for the multiple comparisons for treatment combinations with power as the output.

```
Alpha                              0.05
Error Degrees of Freedom            282
Error Mean Square             2.385761
Critical Value of t            1.96841
Least Significant Difference    0.6206
```

t Grouping	Mean	N	TRT
A	146.9800	48	[1KΩ,EX2]
B	34.0308	48	[1KΩ,EX6]
C	10.5248	48	[1KΩ,EX1]
D	8.7710	48	[1KΩ,EX4]
E	7.5570	48	[1KΩ,EX3]
F	3.6661	48	[1KΩ,EX5]

```
Alpha                              0.05
Error Degrees of Freedom            138
Error Mean Square            0.136126
Critical Value of t            1.97730
Least Significant Difference    0.2106
```

t Grouping	Mean	N	TRT
A	61.9576	24	[10KΩ,EX2]
B	25.5230	24	[10KΩ,EX1]
C	19.7885	24	[10KΩ,EX6]
D	14.4947	24	[10KΩ,EX3]
E	13.1470	24	[10KΩ,EX4]
F	10.2653	24	[10KΩ,EX5]

```
Alpha                              0.05
Error Degrees of Freedom            168
Error Mean Square            0.247116
Critical Value of t            1.97419
Least Significant Difference    0.2577
```

t Grouping	Mean	N	TRT
A	7.1521	29	[100KΩ,EX1]
B	6.4222	29	[100KΩ,EX2]
C	5.0802	29	[100KΩ,EX3]
D	4.3270	29	[100KΩ,EX5]
E	2.7413	29	[100KΩ,EX4]
E			
E	2.6099	29	[100KΩ,EX6]

The SAS output for the multiple comparisons for treatment combinations with impedance as the output.

Alpha	0.05
Error Degrees of Freedom	282
Error Mean Square	104704.5
Critical Value of t	1.96841
Least Significant Difference	130.01

t Grouping	Mean	N	TRT
A	11525.46	48	[1KΩ,EX5]
B	8331.20	48	[1KΩ,EX1]
B			
B	8329.03	48	[1KΩ,EX3]
C	5172.14	48	[1KΩ,EX4]
D	1781.09	48	[1KΩ,EX6]
E	496.08	48	[1KΩ,EX2]

Alpha	0.05
Error Degrees of Freedom	138
Error Mean Square	30262.14
Critical Value of t	1.97730
Least Significant Difference	99.296

t Grouping	Mean	N	TRT
A	13583.51	24	[10KΩ,EX5]
B	11275.94	24	[10KΩ,EX3]
C	8927.80	24	[10KΩ,EX1]
D	5918.45	24	[10KΩ,EX4]
E	1526.34	24	[10KΩ,EX6]
F	290.11	24	[10KΩ,EX2]

APPENDIX B

STATISTICAL DATA ANALYSIS FOR THE ENZYMATIC FUEL CELL

The SAS output for the multiple comparisons of open circuit voltage with respect to flow rate.

Alpha	0.05
Error Degrees of Freedom	6
Error Mean Square	0.00104
Critical Value of t	2.44691
Least Significant Difference	0.0644

t Grouping	Mean	N	TRT
A	0.27679	3	[12ML/MIN]
A			
A	0.26286	3	[25ML/MIN]
A			
A	0.26171	3	[18ML/MIN]

The SAS output for the multiple comparisons of open circuit voltage with respect to concentration.

Alpha	0.05
Error Degrees of Freedom	6
Error Mean Square	0.000683
Critical Value of t	2.44691
Least Significant Difference	0.0522

t Grouping	Mean	N	TRT
A	0.26369	3	[10mM]
A			
A	0.26209	3	[1mM]
A			
A	0.24308	3	[5mM]

The SAS output for the multiple comparisons of open circuit voltage with respect to temperature.

Alpha	0.05
Error Degrees of Freedom	6
Error Mean Square	0.000147
Critical Value of t	2.44691
Least Significant Difference	0.0242

t Grouping	Mean	N	TRT
A	0.309561	3	[20C]
B	0.280755	3	[40C]
B B	0.274619	3	[36C]

The ANOVA results for the load test under different flow conditions. The external loads used were 100Ω, 1000Ω, 5000Ω, 10000Ω.

Current as the parameter

Source	DF	Sum of Squares	Mean Square	F Value	Pr > F
Model	17	260.5857202	15.3285718	8.33	<.0001
Error	18	33.1078497	1.8393250		
Corrected Total	35	293.6935699			

Source	DF	Type I SS	Mean Square	F Value	Pr > F
EXP	2	3.2058941	1.6029470	0.87	0.4353
TRT	2	2.5217849	1.2608925	0.69	0.5165
EXP*TRT	4	4.1723113	1.0430778	0.57	0.6897
LOAD	3	242.4030901	80.8010300	43.93	<.0001
TRT*LOAD	6	8.2826398	1.3804400	0.75	0.6170

Power as the parameter

Source	DF	Sum of Squares	Mean Square	F Value	Pr > F
Model	17	0.00044630	0.00002625	1.51	0.1954
Error	18	0.00031211	0.00001734		
Corrected Total	35	0.00075841			

Source	DF	Type I SS	Mean Square	F Value	Pr > F
EXP	2	0.00000327	0.00000163	0.09	0.9105
TRT	2	0.00001955	0.00000978	0.56	0.5787
EXP*TRT	4	0.00006122	0.00001531	0.88	0.4939
LOAD	3	0.00030163	0.00010054	5.80	0.0059
TRT*LOAD	6	0.00006063	0.00001011	0.58	0.7395

Efficiency as the parameter

Source	DF	Sum of Squares	Mean Square	F Value	Pr > F
Model	17	0.00489051	0.00028768	3.72	0.0041
Error	18	0.00139118	0.00007729		
Corrected Total	35	0.00628169			

Source	DF	Type I SS	Mean Square	F Value	Pr > F
EXP	2	0.00021991	0.00010995	1.42	0.2669
TRT	2	0.00006178	0.00003089	0.40	0.6763
EXP*TRT	4	0.00049259	0.00012315	1.59	0.2191
LOAD	3	0.00396982	0.00132327	17.12	<.0001
TRT*LOAD	6	0.00014641	0.00002440	0.32	0.9204

The SAS output for the multiple comparisons of current with respect to flow rate.

Alpha	0.05
Error Degrees of Freedom	4
Error Mean Square	1.043078
Critical Value of t	2.77645
Least Significant Difference	1.1576

t Grouping	Mean	N	TRT
A	2.3606	12	25ML/MIN
A			
A	2.1095	12	18ML/MIN
A			
A	1.7174	12	12ML/MIN

The SAS output for the multiple comparisons of current with respect to load.

Alpha	0.05
Error Degrees of Freedom	18
Error Mean Square	1.839325
Critical Value of t	2.10092
Least Significant Difference	1.3432

t Grouping	Mean	N	LOAD
A	6.5492	9	100
B	0.7944	9	1000
B			
B	0.5403	9	10000
B			
B	0.3661	9	5000

The SAS output for the multiple comparisons of current with respect to load and flow rate combinations.

Alpha	0.05
Error Degrees of Freedom	22
Error Mean Square	1.694553
Critical Value of t	2.07387
Least Significant Difference	2.2043

t Grouping	Mean	N	GX_HZ
A	7.637	3	100,25ML/MIN
A			
B A	6.950	3	100,18ML/MIN
B			
B	5.060	3	100,12ML/MIN
C	0.836	3	1000,25ML/MIN
C			
C	0.784	3	1000,18ML/MIN
C			
C	0.764	3	1000,12ML/MIN
C			
C	0.650	3	10000,12ML/MIN
C			
C	0.567	3	10000,25ML/MIN
C			
C	0.404	3	10000,18ML/MIN
C			
C	0.403	3	5000,25ML/MIN
C			
C	0.395	3	5000,12ML/MIN
C			
C	0.300	3	5000,18ML/MIN

The SAS output for the multiple comparisons of power with respect to flow rate.

Alpha	0.05
Error Degrees of Freedom	4
Error Mean Square	0.000015
Critical Value of t	2.77645
Least Significant Difference	0.0044

t Grouping	Mean	N	TRT
A	0.004732	12	25ML/MIN
A			
A	0.004213	12	12ML/MIN
A			
A	0.002975	12	18ML/MIN

The SAS output for the multiple comparisons of power with respect to load.

Alpha	0.05
Error Degrees of Freedom	18
Error Mean Square	0.000017
Critical Value of t	2.10092
Least Significant Difference	0.0041

t Grouping	Mean	N	LOAD
A	0.007673	9	100
A			
A	0.005926	9	10000
B	0.001294	9	5000
B			
B	0.001001	9	1000

The SAS output for the multiple comparisons of power with respect to load and flow rate combinations.

Alpha	0.05
Error Degrees of Freedom	22
Error Mean Square	0.000017
Critical Value of t	2.07387
Least Significant Difference	0.007

Means with the same letter are not significantly different.

t Grouping			Mean	N	GX_HZ
	A		0.009698	3	100,25ML/MIN
	A				
B	A		0.008619	3	10000,12ML/MIN
B	A				
B	A	C	0.007583	3	100,18ML/MIN
B	A	C			
B	A	C	0.006510	3	10000,25ML/MIN
B	A	C			
B	A	C	0.005737	3	100,12ML/MIN
B		C			
B		C	0.002648	3	10000,18ML/MIN
		C			
		C	0.001595	3	5000,25ML/MIN
		C			
		C	0.001573	3	5000,12ML/MIN
		C			
		C	0.001123	3	1000,25ML/MIN
		C			
		C	0.000956	3	1000,18ML/MIN
		C			
		C	0.000922	3	1000,12ML/MIN
		C			
		C	0.000713	3	5000,18ML/MIN

The SAS output for the multiple comparisons of efficiency with respect to flow rate.

Alpha	0.05
Error Degrees of Freedom	4
Error Mean Square	0.000123
Critical Value of t	2.77645
Least Significant Difference	0.0126

t Grouping	Mean	N	TRT
A	0.013113	12	25ML/MIN
A			
A	0.013107	12	12ML/MIN
A			
A	0.010331	12	18ML/MIN

The SAS output for the multiple comparisons of efficiency with respect to load.

Alpha	0.05
Error Degrees of Freedom	18
Error Mean Square	0.000077
Critical Value of t	2.10092
Least Significant Difference	0.0087

t Grouping	Mean	N	LOAD
A	0.029877	9	10000
B	0.010240	9	5000
B			
B	0.004650	9	1000
B			
B	0.003969	9	100

The SAS output for the multiple comparisons of efficiency with respect to load and flow rate combinations.

Alpha	0.05
Error Degrees of Freedom	22
Error Mean Square	0.000086
Critical Value of t	2.07387
Least Significant Difference	0.0157

t Grouping	Mean	N	GX_HZ
A	0.034534	3	10000,12ML/MIN
A			
A	0.031571	3	10000,25ML/MIN
A			
B A	0.023526	3	10000,18ML/MIN
B			
B C	0.011393	3	5000,25ML/MIN
B C			
B C	0.010436	3	5000,12ML/MIN
B C			
B C	0.008891	3	5000,18ML/MIN
C			
C	0.004889	3	1000,25ML/MIN
C			
C	0.004722	3	1000,18ML/MIN
C			
C	0.004599	3	100,25ML/MIN
C			
C	0.004337	3	1000,12ML/MIN
C			
C	0.004185	3	100,18ML/MIN
C			
C	0.003122	3	100,12ML/MIN

The ANOVA results for the load test under different concentration conditions.

Current as the parameter

Source	DF	Sum of Squares	Mean Square	F Value	Pr > F
Model	17	285.5972359	16.7998374	402.46	<.0001
Error	18	0.7513770	0.0417432		
Corrected Total	35	286.3486129			

Source	DF	Type I SS	Mean Square	F Value	Pr > F
EXP	2	0.8451953	0.4225976	10.12	0.0011
TRT	2	0.9762882	0.4881441	11.69	0.0006
EXP*TRT	4	1.0276065	0.2569016	6.15	0.0027
LOAD	3	280.7508813	93.5836271	2241.89	<.0001
TRT*LOAD	6	1.9972646	0.3328774	7.97	0.0003

Power as the parameter.

Source	DF	Sum of Squares	Mean Square	F Value	Pr > F
Model	17	0.00029933	0.00001761	23.26	<.0001
Error	18	0.00001363	0.00000076		
Corrected Total	35	0.00031296			

Source	DF	Type I SS	Mean Square	F Value	Pr > F
EXP	2	0.00000436	0.00000218	2.88	0.0821
TRT	2	0.00001155	0.00000577	7.63	0.0040
EXP*TRT	4	0.00001744	0.00000436	5.76	0.0036
LOAD	3	0.00025234	0.00008411	111.10	<.0001
TRT*LOAD	6	0.00001364	0.00000227	3.00	0.0326

Efficiency as the parameter.

Source	DF	Sum of Squares	Mean Square	F Value	Pr > F
Model	17	0.00445426	0.00026202	14.64	<.0001
Error	18	0.00032211	0.00001790		
Corrected Total	35	0.00477637			

Source	DF	Type I SS	Mean Square	F Value	Pr > F
EXP	2	0.00000584	0.00000292	0.16	0.8507
TRT	2	0.00010936	0.00005468	3.06	0.0720
EXP*TRT	4	0.00023453	0.00005863	3.28	0.0349
LOAD	3	0.00388212	0.00129404	72.31	<.0001
TRT*LOAD	6	0.00022240	0.00003707	2.07	0.1081

The SAS output for the multiple comparisons of current with respect to concentration.

Alpha	0.05
Error Degrees of Freedom	4
Error Mean Square	0.256902
Critical Value of t	2.77645
Least Significant Difference	0.5745

t Grouping	Mean	N	TRT
A	2.3887	12	5mM
A			
A	2.1720	12	10mM
A			
A	1.9857	12	1mM

The SAS output for the multiple comparisons of current with respect to load.

Alpha	0.05
Error Degrees of Freedom	18
Error Mean Square	0.041743
Critical Value of t	2.10092
Least Significant Difference	0.2023

t Grouping	Mean	N	LOAD
A	7.00764	9	100
B	0.87736	9	1000
C	0.48967	9	10000
C			
C	0.35396	9	5000

The SAS output for the multiple comparisons of current with respect to load and concentration combinations.

```
Alpha                            0.05
Error Degrees of Freedom           22
Error Mean Square            0.080863
Critical Value of t           2.07387
Least Significant Difference   0.4815
```

t Grouping			Mean	N	GX_HZ
A			7.6279	3	100,5mM
B			7.1317	3	100,10mM
C			6.2633	3	100,1mM
D			0.9813	3	1000,5mM
D					
E	D		0.8693	3	1000,1mM
E	D				
E	D	F	0.7815	3	1000,10mM
E	D	F			
E	D	F	0.5902	3	10000,5mM
E		F			
E		F	0.4678	3	10000,1mM
E		F			
E		F	0.4111	3	10000,10mM
		F			
		F	0.3637	3	5000,10mM
		F			
		F	0.3556	3	5000,5mM
		F			
		F	0.3425	3	5000,1mM

The SAS output for the multiple comparisons of power with respect to concentration.

```
Alpha                            0.05
Error Degrees of Freedom            4
Error Mean Square            4.361E-6
Critical Value of t           2.77645
Least Significant Difference   0.0024
```

t Grouping	Mean	N	TRT
A	0.0043220	12	5mM
A			
A	0.0032682	12	10mM
A			
A	0.0030137	12	1mM

The SAS output for the multiple comparisons of power with respect to load.

Alpha	0.05
Error Degrees of Freedom	18
Error Mean Square	7.571E-7
Critical Value of t	2.10092
Least Significant Difference	0.0009

t Grouping	Mean	N	LOAD
A	0.0077262	9	100
B	0.0038907	9	10000
C	0.0012886	9	1000
C			
C	0.0012332	9	5000

The SAS output for the multiple comparisons of power with respect to load and concentration combinations.

Alpha	0.05
Error Degrees of Freedom	22
Error Mean Square	1.412E-6
Critical Value of t	2.07387
Least Significant Difference	0.002

t Grouping	Mean	N	GX_HZ
A	0.0090600	3	100,5mM
A			
B A	0.0079709	3	100,10mM
B			
B C	0.0061477	3	100,1mM
C			
D C	0.0054367	3	10000,5mM
D			
D E	0.0035458	3	10000,1mM
E			
F E	0.0026896	3	10000,10mM
F			
F	0.0015294	3	1000,5mM
F			
F	0.0013089	3	5000,10mM
F			
F	0.0012621	3	5000,5mM
F			
F	0.0012328	3	1000,1mM
F			
F	0.0011285	3	5000,1mM
F			
F	0.0011035	3	1000,10mM

The SAS output for the multiple comparisons of efficiency with respect to concentration.

```
Alpha                             0.05
Error Degrees of Freedom             4
Error Mean Square             0.000059
Critical Value of t            2.77645
Least Significant Difference    0.0087


t Grouping           Mean      N    TRT

         A      0.015006     12    5mM
         A
         A      0.011868     12    1mM
         A
         A      0.010929     12    10mM
```

The SAS output for the multiple comparisons of efficiency with respect to load.

```
Alpha                             0.05
Error Degrees of Freedom            18
Error Mean Square             0.000018
Critical Value of t            2.10092
Least Significant Difference    0.0042

Means with the same letter are not significantly different.

t Grouping           Mean      N    LOAD

         A      0.030114      9    10000

         B      0.010580      9    5000

         C      0.005382      9    1000
         C
         C      0.004329      9    100
```

The SAS output for the multiple comparisons of efficiency with respect to load and concentration combinations.

```
Alpha                             0.05
Error Degrees of Freedom            22
Error Mean Square             0.000025
Critical Value of t            2.07387
Least Significant Difference    0.0085
```

Means with the same letter are not significantly different.

t Grouping	Mean	N	GX_HZ
A	0.038334	3	10000,5mM
B	0.027892	3	10000,1mM
B			
B	0.024117	3	10000,10mM
C	0.010702	3	5000,10mM
C			
C	0.010585	3	5000,1mM
C			
C	0.010453	3	5000,5mM
C			
C	0.006238	3	1000,5mM
C			
C	0.005253	3	1000,1mM
C			
C	0.004997	3	100,5mM
C			
C	0.004654	3	1000,10mM
C			
C	0.004245	3	100,10mM
C			
C	0.003744	3	100,1mM

The ANOVA results for the load test under different temperature conditions.

Current as the parameter

Source	DF	Sum of Squares	Mean Square	F Value	Pr > F
Model	17	194.9840779	11.4696516	72.68	<.0001
Error	18	2.8405321	0.1578073		
Corrected Total	35	197.8246100			

Source	DF	Type I SS	Mean Square	F Value	Pr > F
EXP	2	0.2671354	0.1335677	0.85	0.4453
TRT	2	7.7682427	3.8841213	24.61	<.0001
EXP*TRT	4	0.3696321	0.0924080	0.59	0.6772
LOAD	3	168.9260863	56.3086954	356.82	<.0001
TRT*LOAD	6	17.6529815	2.9421636	18.64	<.0001

Power as the parameter

Source	DF	Sum of Squares	Mean Square	F Value	Pr > F
Model	17	0.00018326	0.00001078	5.68	0.0003
Error	18	0.00003416	0.00000190		
Corrected Total	35	0.00021743			

Source	DF	Type I SS	Mean Square	F Value	Pr > F
EXP	2	0.00000596	0.00000298	1.57	0.2350
TRT	2	0.00002573	0.00001287	6.78	0.0064
EXP*TRT	4	0.00000403	0.00000101	0.53	0.7144
LOAD	3	0.00010742	0.00003581	18.87	<.0001
TRT*LOAD	6	0.00004011	0.00000669	3.52	0.0175

Efficiency as the parameter

Source	DF	Sum of Squares	Mean Square	F Value	Pr > F
Model	17	0.00113780	0.00006693	4.20	0.0021
Error	18	0.00028665	0.00001592		
Corrected Total	35	0.00142445			

Source	DF	Type I SS	Mean Square	F Value	Pr > F
EXP	2	0.00022279	0.00011140	7.00	0.0057
TRT	2	0.00007574	0.00003787	2.38	0.1212
EXP*TRT	4	0.00005331	0.00001333	0.84	0.5195
LOAD	3	0.00074183	0.00024728	15.53	<.0001
TRT*LOAD	6	0.00004412	0.00000735	0.46	0.8274

The SAS output for the multiple comparisons of current with respect to load .

Alpha	0.05
Error Degrees of Freedom	18
Error Mean Square	0.157807
Critical Value of t	2.10092
Least Significant Difference	0.3934

t Grouping	Mean	N	LOAD
A	5.4374	9	100
B	0.7426	9	1000
C	0.3461	9	5000
C			
C	0.2677	9	10000

The SAS output for the multiple comparisons of current with respect to temperature.

Alpha	0.05
Error Degrees of Freedom	4
Error Mean Square	0.092408
Critical Value of t	2.77645
Least Significant Difference	0.3446

t Grouping	Mean	N	TRT
A	2.0563	12	36C
A			
A	1.9967	12	40C
B	1.0424	12	20C

The SAS output for the multiple comparisons of current with respect to load and temperature combinations.

Alpha	0.05
Error Degrees of Freedom	22
Error Mean Square	0.145917
Critical Value of t	2.07387
Least Significant Difference	0.6468

t Grouping	Mean	N	GX_HZ
A	6.8288	3	100,36C
A			
A	6.4022	3	100,40C
B	3.0814	3	100,20C
C	0.8251	3	1000,40C
C			
C	0.7844	3	1000,36C
C			
C	0.6182	3	1000,20C
C			
C	0.4428	3	5000,40C
C			
C	0.3816	3	5000,36C
C			
C	0.3167	3	10000,40C
C			
C	0.2562	3	10000,20C
C			
C	0.2303	3	10000,36C
C			
C	0.2140	3	5000,20C

The SAS output for the multiple comparisons of power with respect to load .

Alpha	0.05
Error Degrees of Freedom	18
Error Mean Square	1.898E-6
Critical Value of t	2.10092
Least Significant Difference	0.0014

t Grouping	Mean	N	LOAD
A	0.0051587	9	100
B	0.0013082	9	10000
B			
B	0.0012680	9	5000
B			
B	0.0009672	9	1000

The SAS output for the multiple comparisons of power with respect to temperature.

Alpha	0.05
Error Degrees of Freedom	4
Error Mean Square	1.008E-6
Critical Value of t	2.77645
Least Significant Difference	0.0011

Means with the same letter are not significantly different.

t Grouping	Mean	N	TRT
A	0.0028009	12	40C
A			
A	0.0027454	12	36C
B	0.0009803	12	20C

The SAS output for the multiple comparisons of power with respect to load and temperature combinations.

Alpha	0.05
Error Degrees of Freedom	22
Error Mean Square	1.736E-6
Critical Value of t	2.07387
Least Significant Difference	0.0022

t Grouping	Mean	N	GX_HZ
A	0.007494	3	100,36C
A			
A	0.006447	3	100,40C
B	0.001879	3	5000,40C
B			
B	0.001817	3	10000,40C
B			
B	0.001544	3	5000,36C
B			
B	0.001535	3	100,20C
B			
B	0.001199	3	10000,20C
B			
B	0.001061	3	1000,40C
B			
B	0.001034	3	1000,36C
B			
B	0.000909	3	10000,36C
B			
B	0.000806	3	1000,20C
B			
B	0.000380	3	5000,20C

The SAS output for the multiple comparisons of efficiency with respect to load .

Alpha	0.05
Error Degrees of Freedom	18
Error Mean Square	0.000016
Critical Value of t	2.10092
Least Significant Difference	0.004

t Grouping	Mean	N	LOAD
A	0.014396	9	10000
B	0.009312	9	5000
C	0.004078	9	1000
C			
C	0.003023	9	100

The SAS output for the multiple comparisons of efficiency with respect to temperature.

Alpha	0.05
Error Degrees of Freedom	4
Error Mean Square	0.000013
Critical Value of t	2.77645
Least Significant Difference	0.0041

t Grouping	Mean	N	TRT
A	0.009312	12	40C
A			
A	0.007998	12	36C
A			
A	0.005796	12	20C

The SAS output for the multiple comparisons of efficiency with respect to load and temperature combinations.

Alpha	0.05
Error Degrees of Freedom	22
Error Mean Square	0.000015
Critical Value of t	2.07387

Least Significant Difference 0.0067

t Grouping			Mean	N	GX_HZ
	A		0.017215	3	10000,40C
	A				
	A		0.012990	3	10000,36C
	A				
	A		0.012982	3	10000,20C
	A				
B	A		0.011919	3	5000,40C
B	A				
B	A	C	0.010608	3	5000,36C
B		C			
B	D	C	0.005410	3	5000,20C
	D	C			
	D	C	0.004544	3	1000,40C
	D	C			
	D	C	0.004463	3	1000,36C
	D				
	D		0.003930	3	100,36C
	D				
	D		0.003571	3	100,40C
	D				
	D		0.003227	3	1000,20C
	D				
	D		0.001567	3	100,20C